CHAPTER 5 : The Coastal Discontinuity Model

Chapter authors: Dr R J Barthelmie (Risø National Laboratory) & Drs. J.P. Coelingh and Dr. L. Folkerts (Ecofys)

5.1 Coastal Discontinuity - theoretical background

The initial focus of this part of the project was to develop and evaluate a coastal model which uses standard meteorological measurements (wind speed, temperature profiles, sea temperature) to estimate stability parameters for use in predicting wind speed profiles. The importance of stability that is addressed within the Coastal Discontinuity Model (CDM) is that:

1) In non-neutral conditions wind speed profiles are distorted from logarithmic. WAsP assumes a slightly stable profile on average which is reasonable for land areas but has not been fully evaluated for all offshore areas. Most of the sites for which full analysis has been conducted in the Baltic and Denmark have been shown to be more frequently stable than unstable (Barthelmie *et al.*, 1999). However off the coast of the Netherlands sites were found to be slightly unstable on average (Coelingh *et al.*, 1998), (Coelingh *et al.*, 1996). Stability has been shown to significant impact the wind speed distribution as flow moves offshore (Pryor and Barthelmie, 1998).

   To calculate the Monin-Obukhov length, heat and momentum fluxes should be measured using a sonic anemometer. Since these data are not available for most offshore sites, fluxes offshore are estimated here using temperature profiles calculated from the difference between air and sea temperature. The routines used were developed at the Royal Netherlands Meteorological Institute (Beljaars *et al.*, 1989). This methodology has the potential to create a large temperature difference since different instruments and techniques were used to determine air and sea temperatures. A comparison of fluxes estimated using the (Beljaars *et al.*, 1989)'s routines and calculated from measured fluxes is given in Section 5.4. The routines have been shown to give good agreement with measured fluxes based on a measured temperature difference. However, the measured temperature difference is a precise measurement while the temperature difference calculated from measured air and sea temperatures is not, unless the two temperature sensors are calibrated together. Errors in temperature measurements are of the same order as the temperature difference. If the temperature datasets are derived from different sources then the errors arising from calculating the temperature difference can be substantial.

2) Internal Boundary Layer (IBL) growth varies under different stability conditions. In stable conditions offshore the IBL grows slowly and can remain below 100 m for considerable distances inhibiting momentum exchange and impacting the wind speed profile (Garratt and Ryan, 1989), (Smedman *et al.*, 1997), (Van Wijk *et al.*, 1990a). Conversely in unstable conditions the IBL grows quickly rapidly attaining equilibrium. To calculate the IBL height the formula presented by (Bergstrom *et al.*, 1988) is used which shows good agreement (Barthelmie and Palutikof, 1996) with that developed by (Van Wijk *et al.*, 1990a). The three layer model used by Risø is based on the same principles as those used in (Van Wijk *et al.*, 1990b), (Van Wijk *et al.*, 1990a), (Bergstrom *et al.*, 1988) focused on prediction on wind speed profiles moving offshore. The three-layer concept involves a lower layer that is in equilibrium with the sea surface, an upper layer which is in equilibrium with the overlying air and an adjustment or blending layer where the two air masses meet.

Stability corrections can be calculated based on Monin-Obukhov similarity theory (see e.g. (Van Wijk *et al.*, 1990b) where the Monin-Obukhov length, L, is given by:

$$L = -\frac{u_*^3}{k(g/\theta)\overline{w'\theta'}} \tag{5.1}$$

where θ is the potential temperature,
k is the von Karman constant,
g is acceleration due to gravity,
u_* is the friction velocity, and
w is the vertical velocity.

Incorporating a stability correction into the logarithmic wind speed profile, the wind speed, U at height, z is calculated by:

$$U = \frac{u_*}{k}\left(\ln\left(\frac{z}{z_o}\right) - \Psi\left(\frac{z}{L}\right) \right) \quad (5.2)$$

where z is the height,
z_0 is the roughness length, and
Ψ is the stability correction to the wind speed and is given by:

$$\Psi = -5\left(\frac{z}{L}\right) \text{ for stable conditions (L>0)} \quad (5.3)$$

and

$$\Psi = 2\ln\left(\frac{1+x}{2}\right) + \ln\left(\frac{1+x^2}{2}\right) - 2\tan^{-1}x + \frac{\Pi}{2} \text{ for unstable conditions (L<0)} \quad (5.4)$$

where:

$$x = \left(1 - 16\left(\frac{z}{L}\right)\right)^{\frac{1}{4}} \quad (5.5)$$

Thus, the magnitude of stability correction to a near-neutral wind speed profile ($\Psi(z/L)$) depends on whether conditions are stable or unstable (the absolute value of the stability correction is larger if conditions are stable) and by how much conditions deviate from near-neutral (as defined by the Monin-Obukhov length). As conditions approach neutral, the Monin-Obukhov length increases, conversely as conditions become more unstable or more stable the Monin-Obukhov length tends towards zero. Note that corrections are subtracted from the near-neutral wind speed, hence the net impact is that corrections are negative in unstable conditions and positive in stable conditions. The wind speed also depends on the ratio u_*/k and u_* is typically lower when conditions are non-neutral.

5.2 CDM Modelling and results

5.2.1 Outline of the CDM approach: geostrophic version

The intention of this part of the project was to modify WAsP derived wind speed profiles to take account of stability effects calculated from air and sea temperature databases. Since WAsP derived wind speeds were not initially available, the first version of the Coastal Discontinuity Model was developed and applied using geostrophic wind speeds as input (Figure 5-1). This is referred to in the following as the GEO-CDM. The following steps were required:

1. Grid points for geostrophic wind speeds were initially latitude and longitude but since fetch (distance to the coast) is required for calculating the height of the internal boundary layer (IBL), the co-ordinates were transformed to Universal Transverse Mercator (UTM). Since the area of offshore wind speeds required crosses several UTM zones, the area has been divided into seven distinct regions as shown in Figure 5-2 to reduce errors associated with the projection. Although no difficulties are anticipated with the reintegration of these areas, small overlaps have been introduced for checking purposes.
2. Coastline data for each area were transformed to UTM co-ordinates.
3. A program was written to calculate the minimum fetch distance for each geostrophic data point offshore. Each pair of geostrophic co-ordinates is given a minimum fetch distance in one of 12 directional bins.
4. To input geostrophic wind data, a linking file was developed to provide latitude, longitude, UTM co-ordinates and filenames for all the geostrophic wind data.
5. The CDM reads in the geostrophic wind speed and data for each grid point. The program searches the fetch file to ensure the co-ordinates are present and determines the minimum fetch distance for each direction.
6. For each geostrophic wind speed value the program determines whether the wind direction is from land, sea or has a mixed fetch over which an internal boundary layer will develop. If the fetch is uniform (either land or sea) friction velocity is used to generate a neutral wind speed profile and the ageostrophic angle is calculated which is used to correct the near surface wind directions. The friction velocity is calculated for a range of geostrophic wind speeds between 3 and 40 m/s. Offshore variable roughness is calculated based on the Charnock equation (Charnock, 1955). This means that the friction velocity offshore is under-estimated in low wind speeds (below about 4 m/s). The constant used in the Charnock equation is 0.018 which is suitable for coastal areas.
7. If an IBL is present Bergström's formula (Bergström *et al.*, 1988) is used to determine the neutral IBL height at the geostrophic grid location. This formulation for the IBL height has been compared with that of (Van Wijk *et al.*, 1990) and is found to produce similar predictions for the IBL height (Barthelmie and Palutikof, 1996). Beneath this height the equilibrium neutral sea profile is used, above this height the equilibrium land wind speed profile is used. Here we use a three layer IBL formulation (Figure 5-3) where the height of the adjustment layer is 20% of the IBL. The effect of varying the depth of this layer is shown in Figure 5-4. Finally

for each offshore grid point a wind speed profile is calculated which depends only on the geostrophic wind speed distribution and the distance of the point to the coastline in each direction.

8. The CDM can be used to either give near-neutral predictions if no air/sea temperatures or temperature profiles are available or the Monin-Obukhov length (stability parameter) is determined according to the sea surface temperature, an air temperature and the wind speed and direction. The CDM has been applied in each area and gives results which should be directly comparable with those of the WAsP model (Mortensen *et al.*, 1993). WAsP and the CDM are based on similar principles. Major differences between WAsP and the version of the CDM which has been applied offshore are:
    - WAsP makes adjustments to the wind speed profile offshore based on the assumption that the wind speed profile in the surface layer (up to approximately first 100m) is slightly stable.
    - CDM has variable roughness offshore which is dependent on the wind speed.
    - WAsP calculates a mean stability correction to the wind speed profile depending whether the location is on- or offshore. The CDM uses the time series data to calculate the stability parameter and correct the wind speed profile for each observation which is then averaged. These two approaches do not give identical results since a mean stability correction is smaller than the average correction as calculated from individual wind speed profiles.

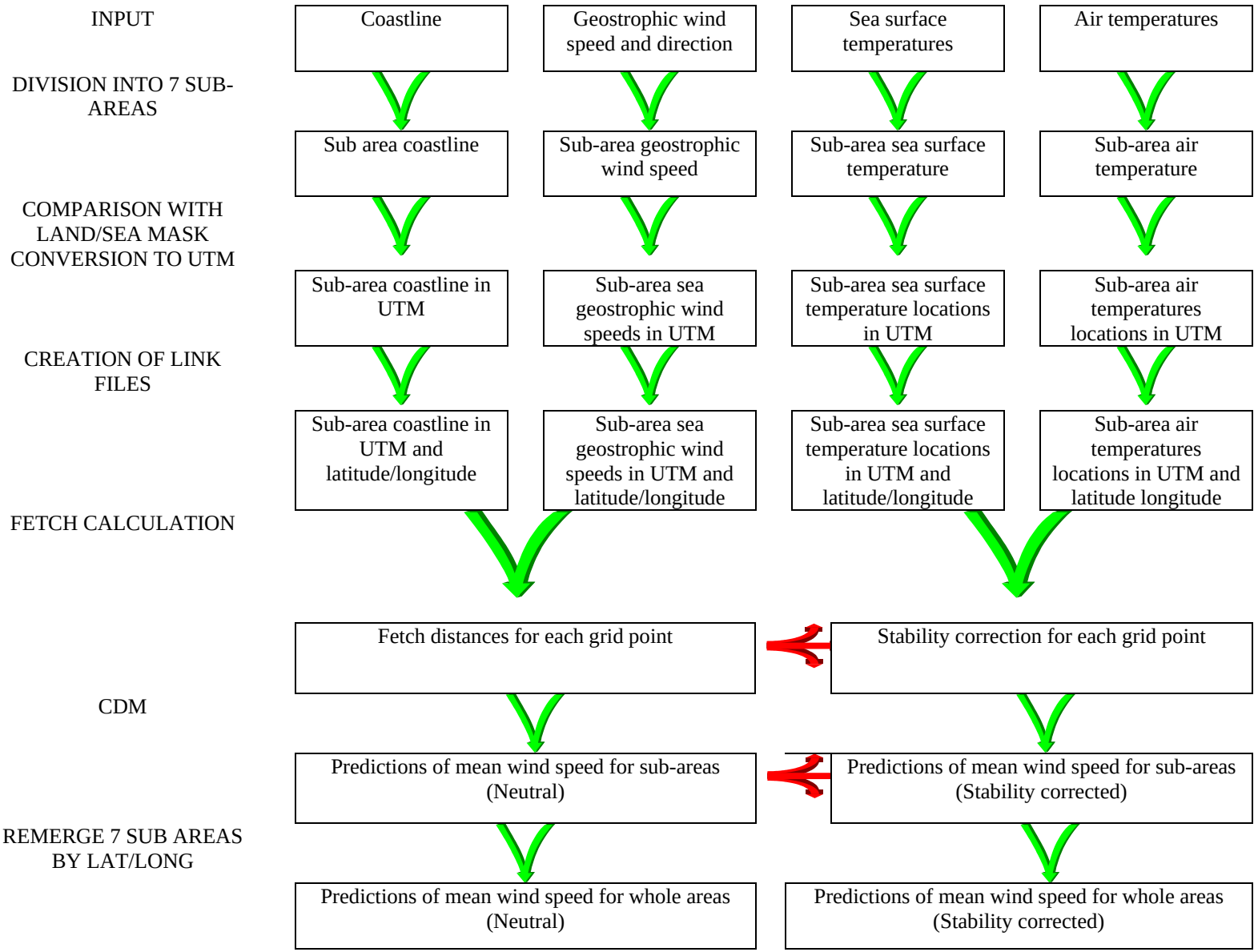

Figure 5-1. Sketch of CDM - geostrophic methodology

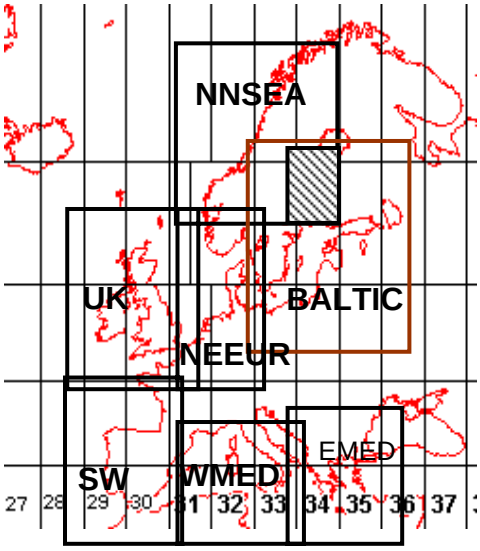

1. BALTIC: Baltic
2. NNSEA: Northern North Sea
3. UK: UK
4. NEEUR: Northeast Europe (as zone 32)
5. SWEUR: Southwest Europe
6. WMED: Western Mediterranean
7. EMED: Eastern Mediterranean

Figure 5-2. Subdivision into seven areas for application of the CDM

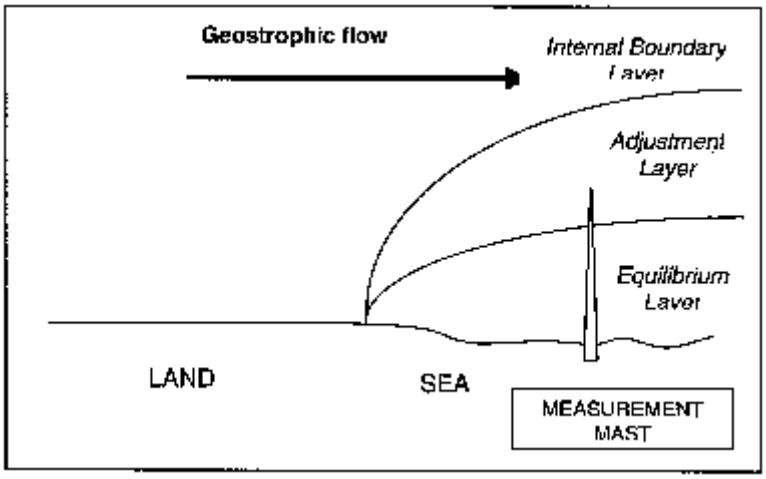

Figure 5-3. Concept of the three-layer IBL

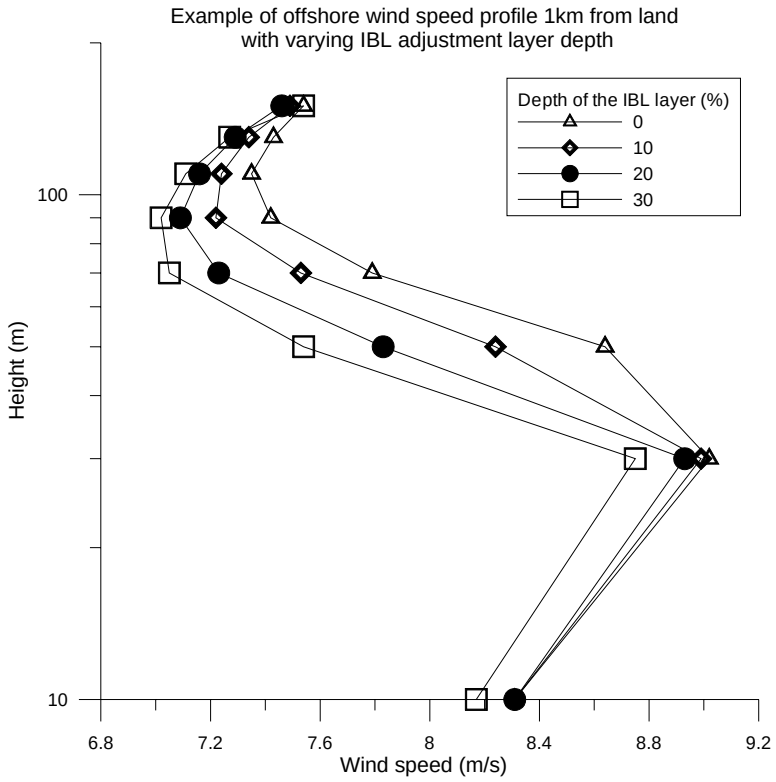

Figure 5-4. Effect of the depth of the adjustment zone (shown as a percentage of the IBL depth) on interpolation on predicted wind speed profiles

5.2.2 Application and assessment of the GEO-CDM

Figure 5-5a shows 1997 geostrophic wind speeds for the European region. These follow the general pattern expected since for this area on average. Highest geostrophic wind speeds occur in the northwest decreasing towards the southeast (Troen and Petersen, 1989). In 1997 highest geostrophic wind speeds exceeding 12 m/s occurred in the northwest and lowest geostrophic wind speeds occurred in the Mediterranean.

Simulations with the GEO-CDM (neutral formulation) appear to give reliable and consistent results for near-surface wind speed profiles (Figure 5-5b) since near-surface wind speeds follow the general pattern given by geostrophic wind speeds. Wind speeds in areas which are strongly affected by thermal flows such as the Baltic show lower wind speeds than anticipated.

Figure 5-6 shows geostrophic and predicted near-surface wind speeds (heights from 10m to 150 m) from the neutral GEO-CDM formulation. One feature that appears consistently in the model results is high near-surface wind speed along the coast of the former Yugoslavia. This results from high geostrophic wind speeds in this area and strong coupling to near-surface winds. As has been noted previously this coupling between geostrophic and near-surface wind speeds is not realistic in Mediterranean areas.

Figure 5-7 shows predicted near-surface wind speeds (heights from 10m to 150 m) with stability correction. In the Baltic the dominance of stable conditions leads to positive corrections to near-surface winds speeds (Barthelmie, 1999b). In addition in these offshore regions are subject to low-level jets at heights below 200 m which are expected to significantly impact the wind resource (Smedman *et al.*, 1996). In the Mediterranean local wind speeds are expected to be impacted by local and regional thermal flows which can only be captured by mesoscale models.

The effect of stability on wind speed profiles is shown in Figures 5-8 and 5-9. The magnitude of the correction to the profile is large when the Monin-Obukhov is small and rapidly decreases as conditions tend toward neutral (i.e. the Monin-Obukhov length exceeds $\pm$1000 m). The mean Monin-Obukhov length for most of European offshore areas (Figure 5-9) is close to neutral. This is expected since stable and unstable conditions tend to balance out over the course of the year. The CDM uses time series data to calculate the stability correction to each wind speed profile and does not use the stability parameter to calculate a mean correction to the profile. Note that some areas are unstable on average (northeast North Sea and parts of the Mediterranean) while some (central Baltic) are stable.
In the following sections two additional parameterisation of the CDM were considered, the first is the role of variable roughness offshore and the second is the width of the coastal zone.

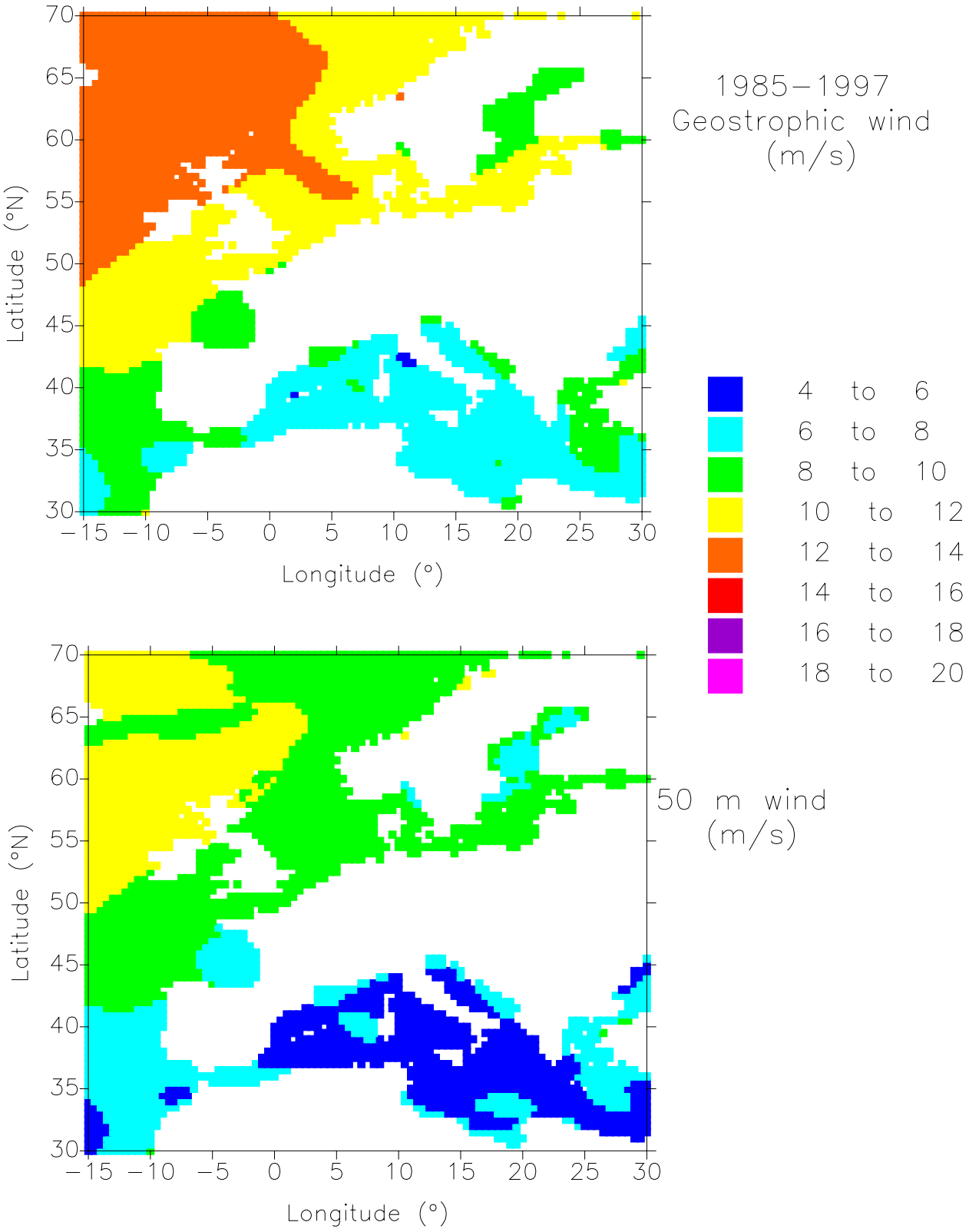

Figure 5-5. a) Mean geostrophic wind speed (1985-1997) and b) GEO-CDM predictions of 50 m wind speeds (neutral formulation).

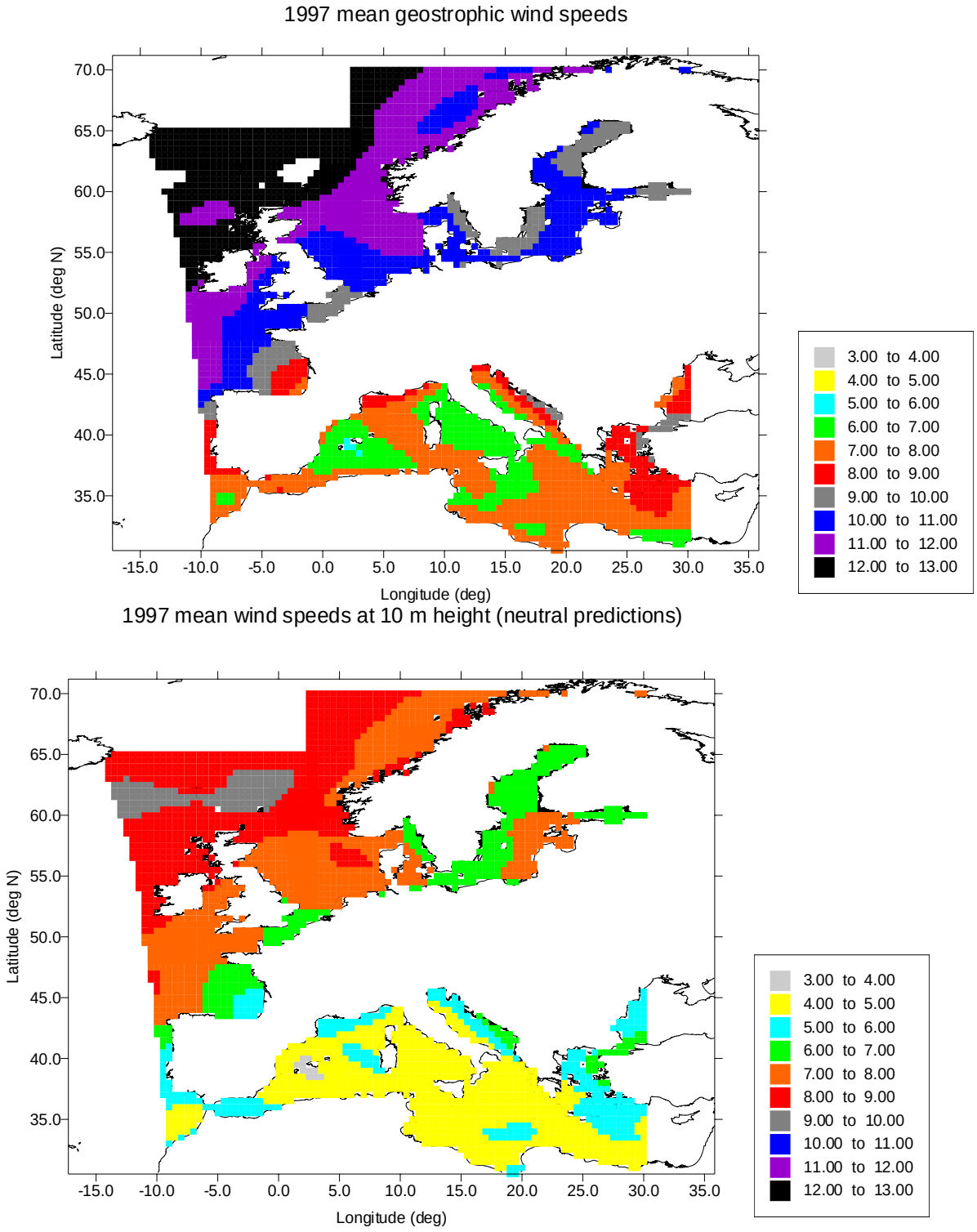

Figure 5-6. Geostrophic wind speeds in 1997 and neutral predictions of wind speed from 10m to 150m above the surface.

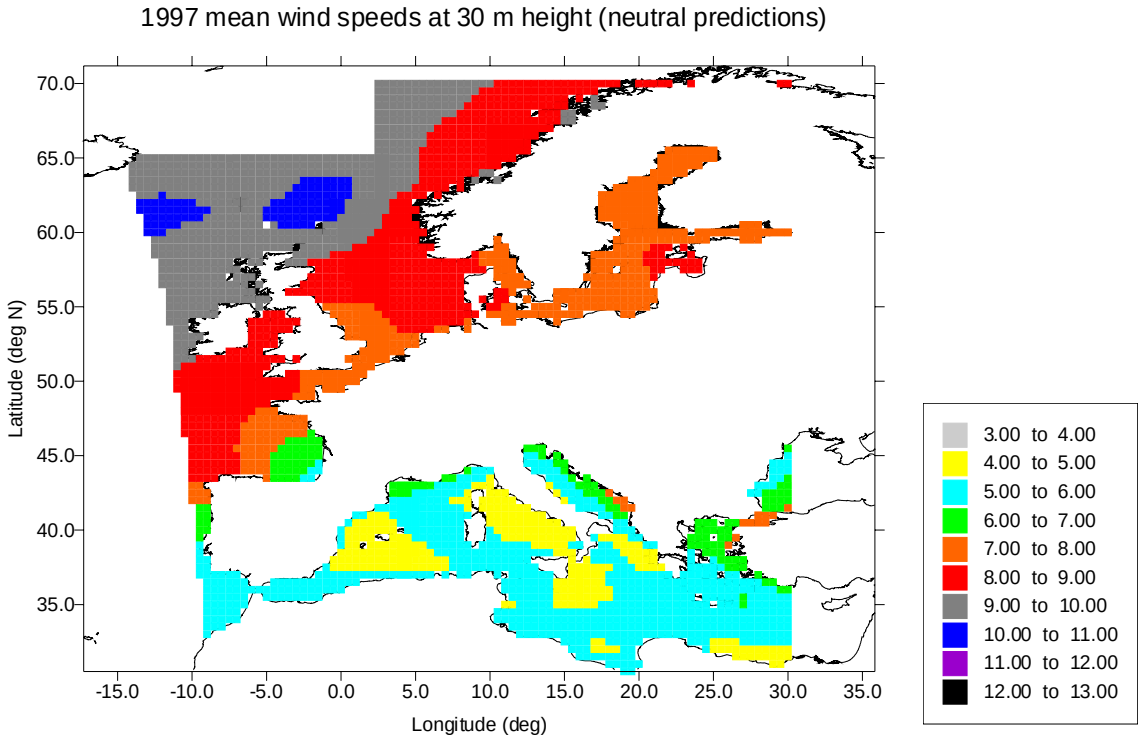

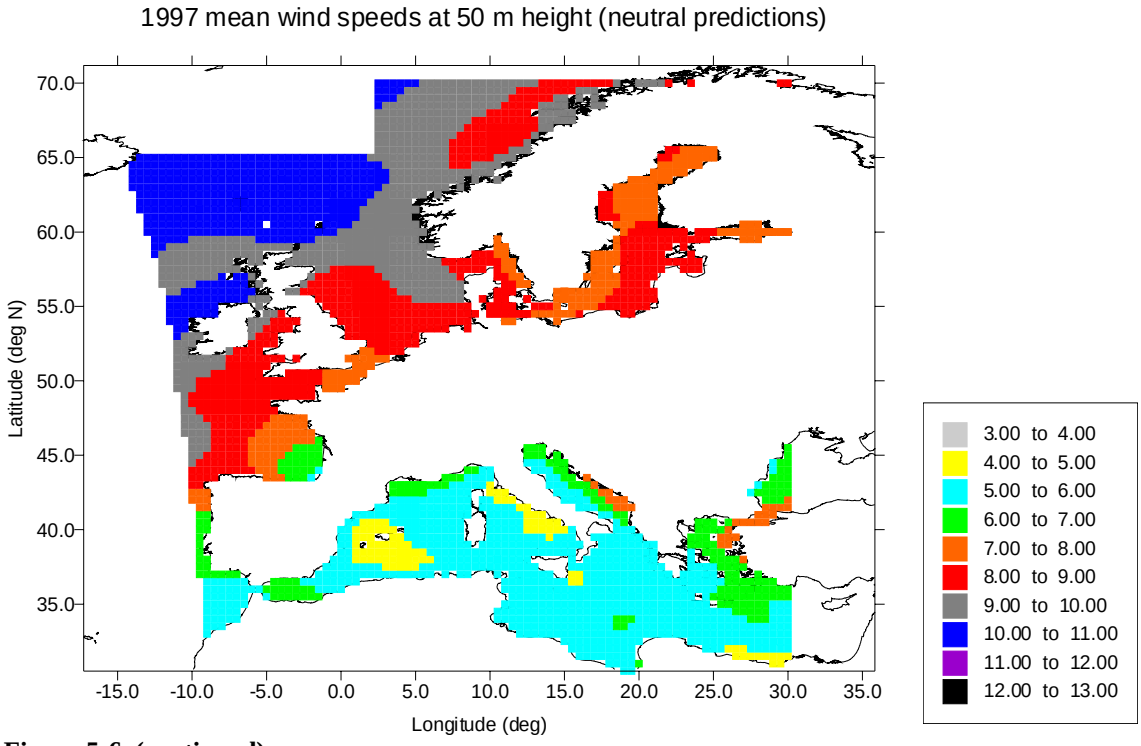

Figure 5-6. (continued).

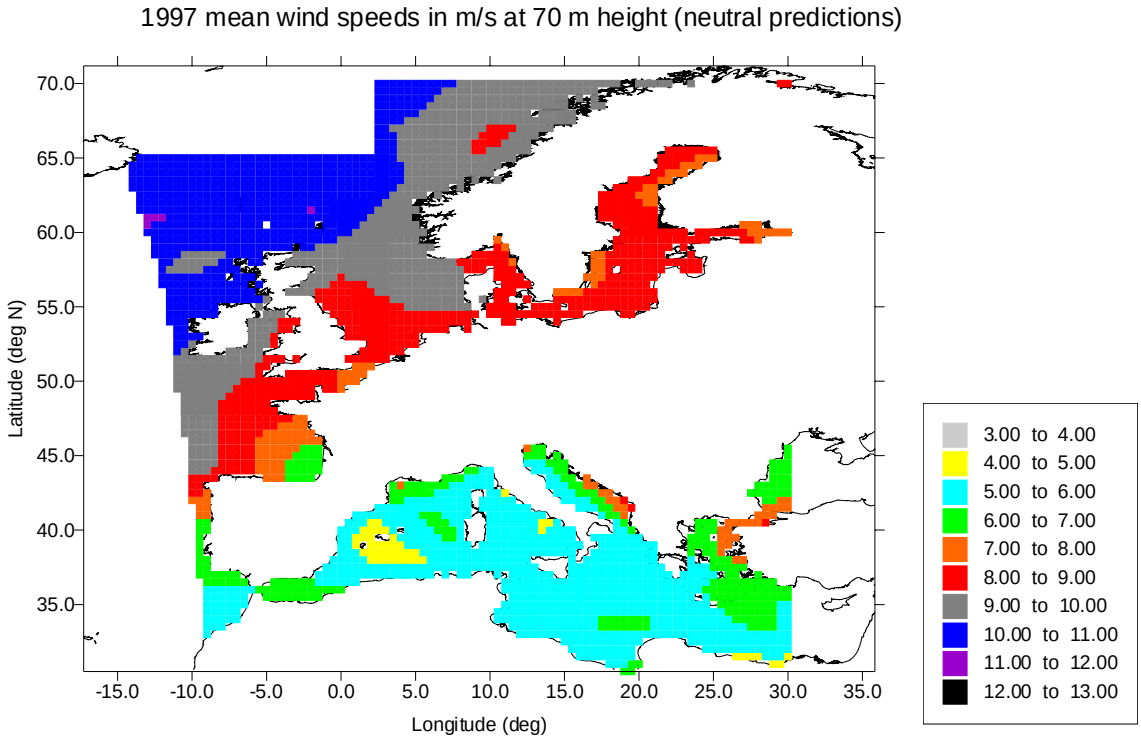

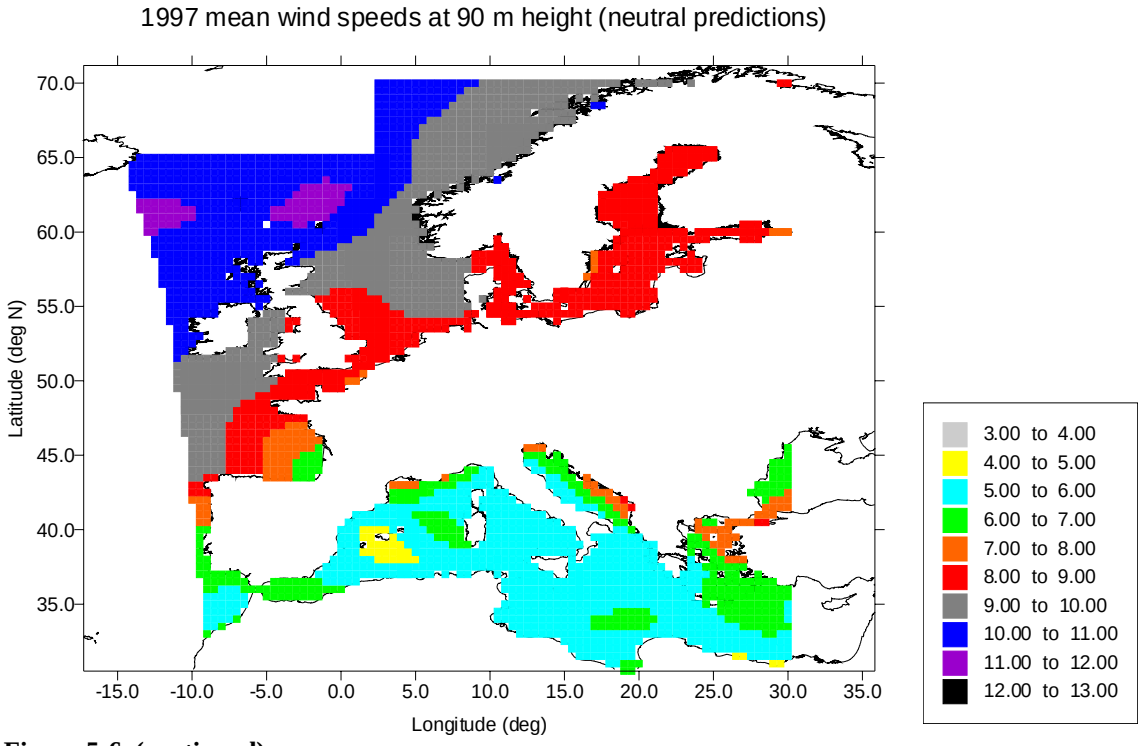

Figure 5-6. (continued).

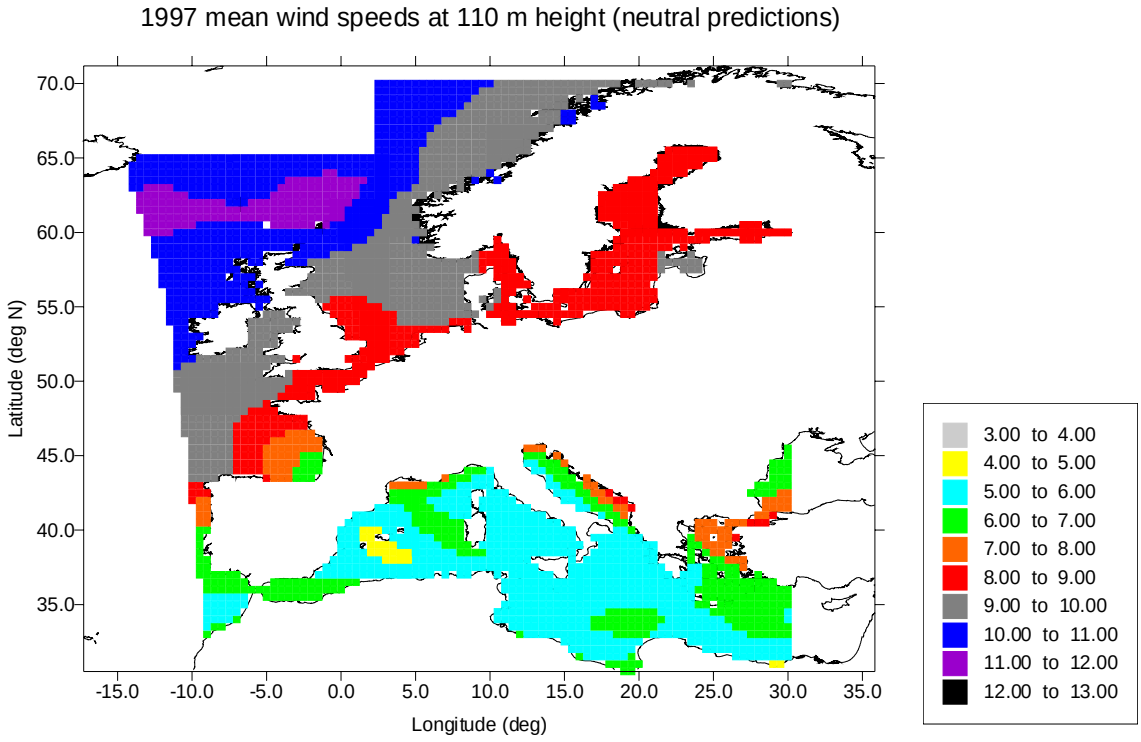

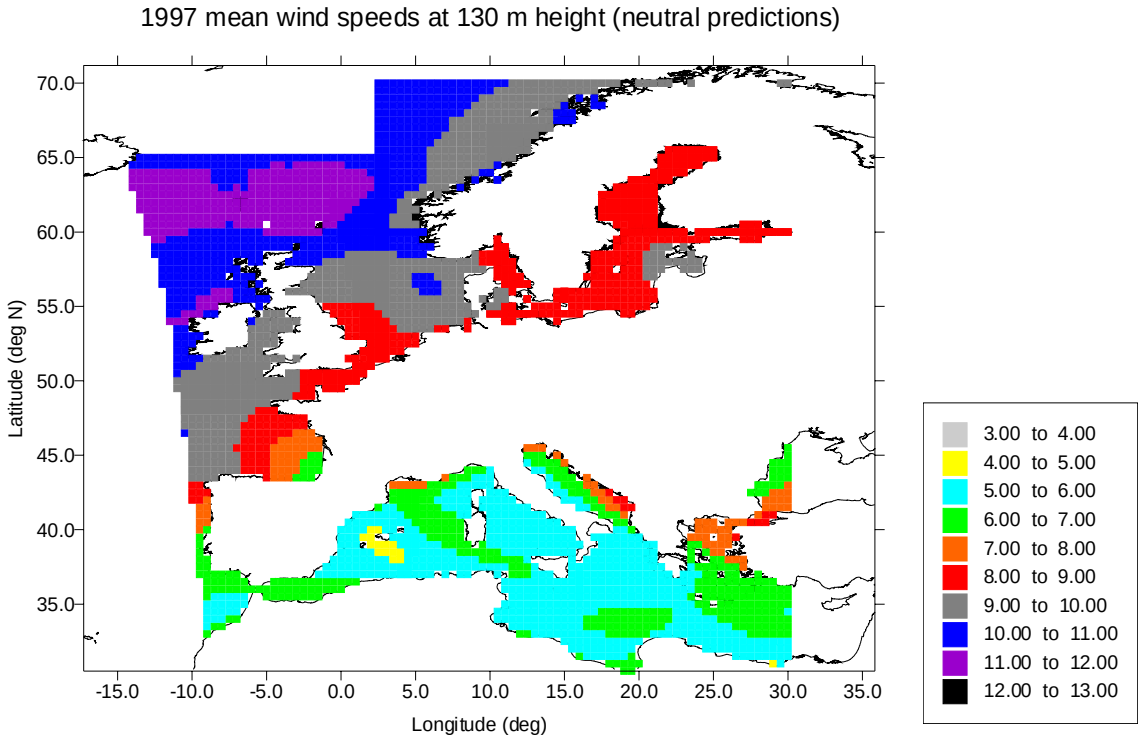

Figure 5-6. (continued).

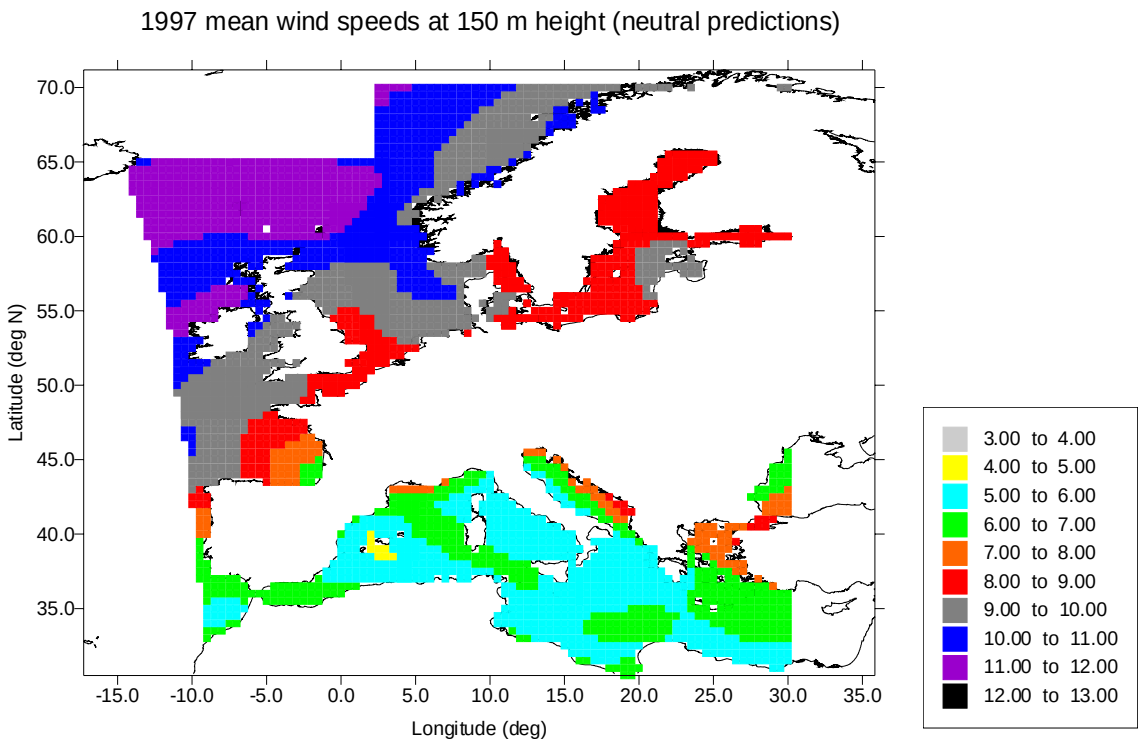

Figure 5-6. (continued).

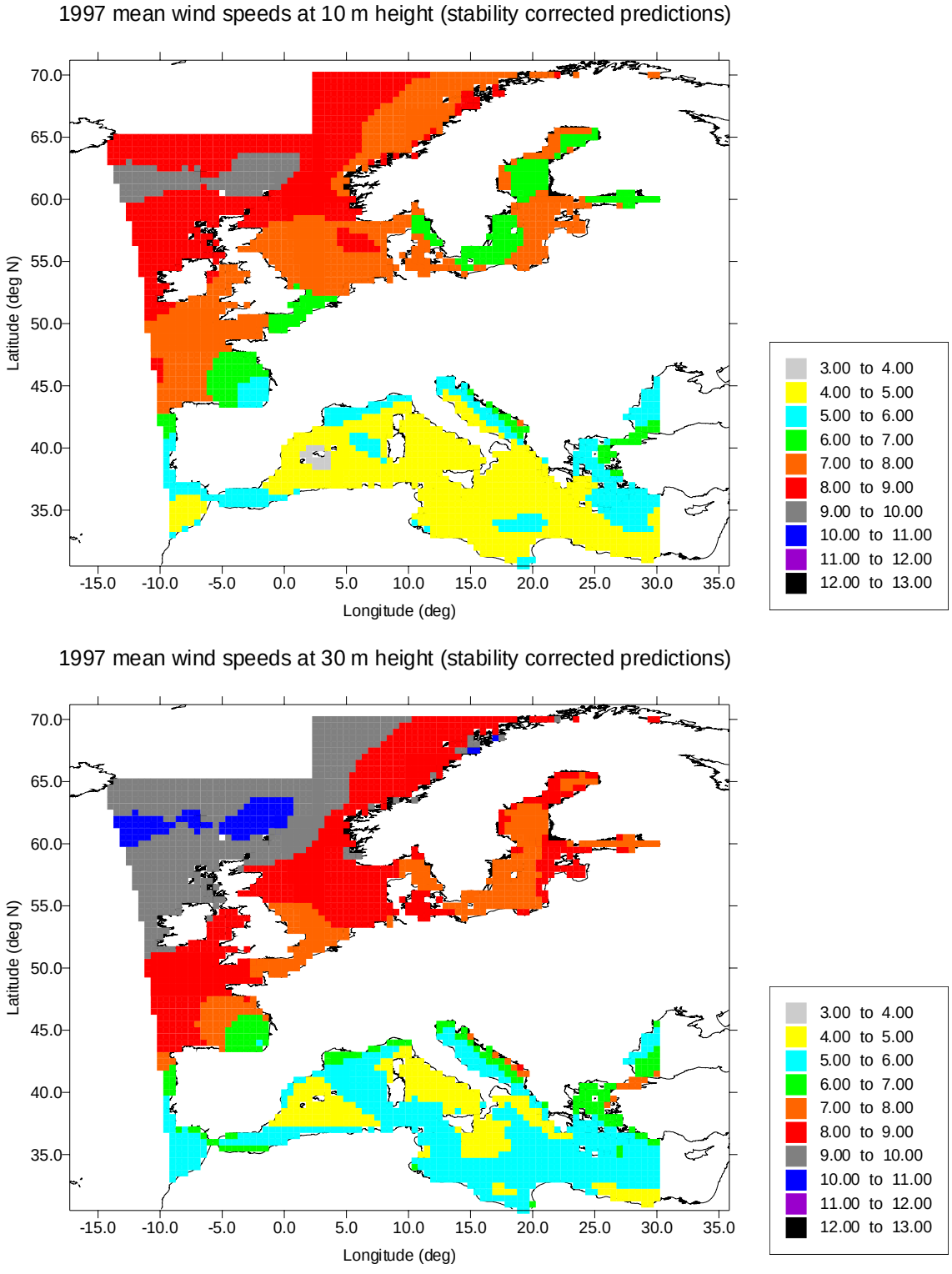

Figure 5-7. Stability corrected near-surface wind speeds from the GEO-CDM (m/s).

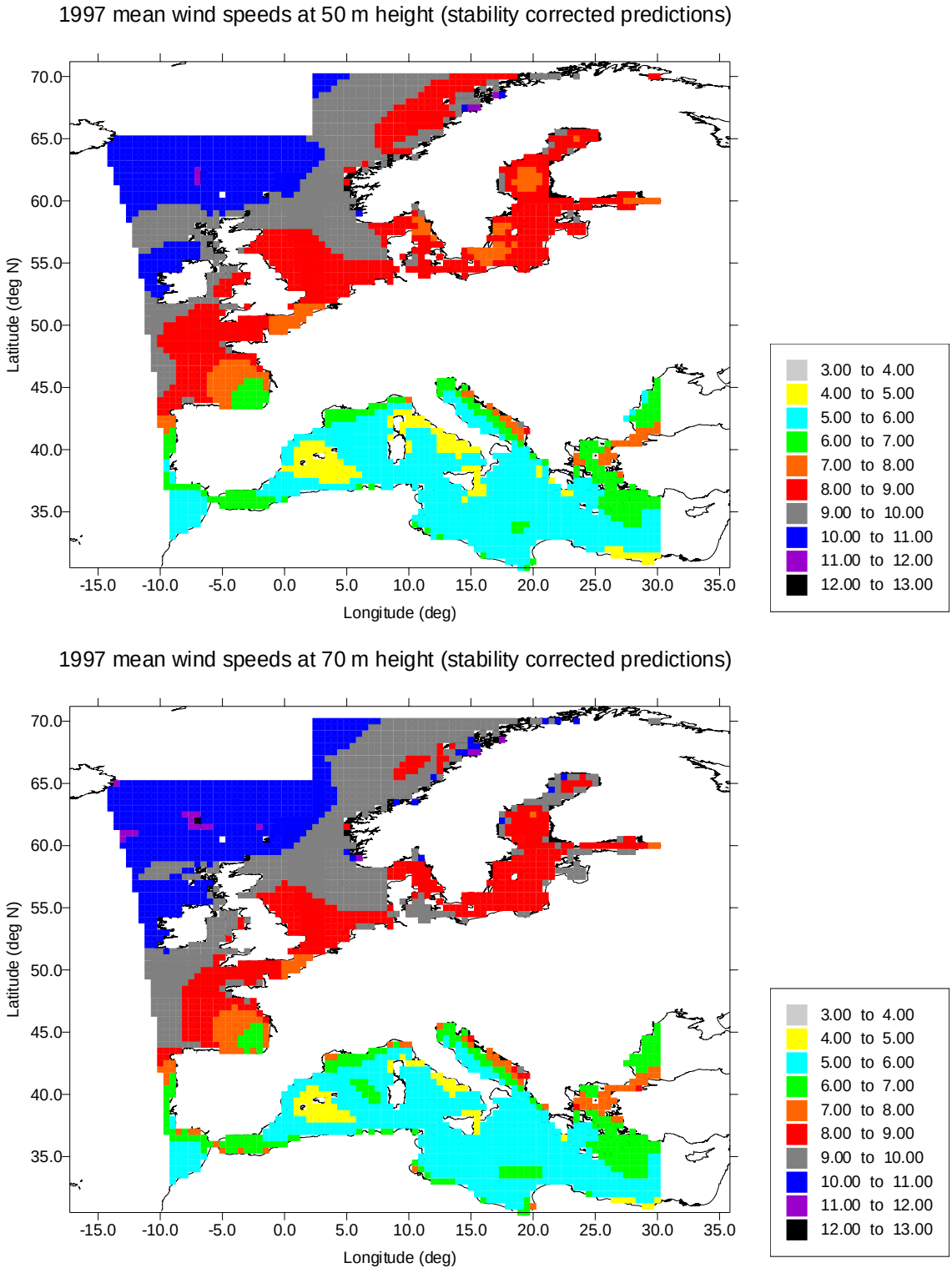

Figure 5-7. (continued).

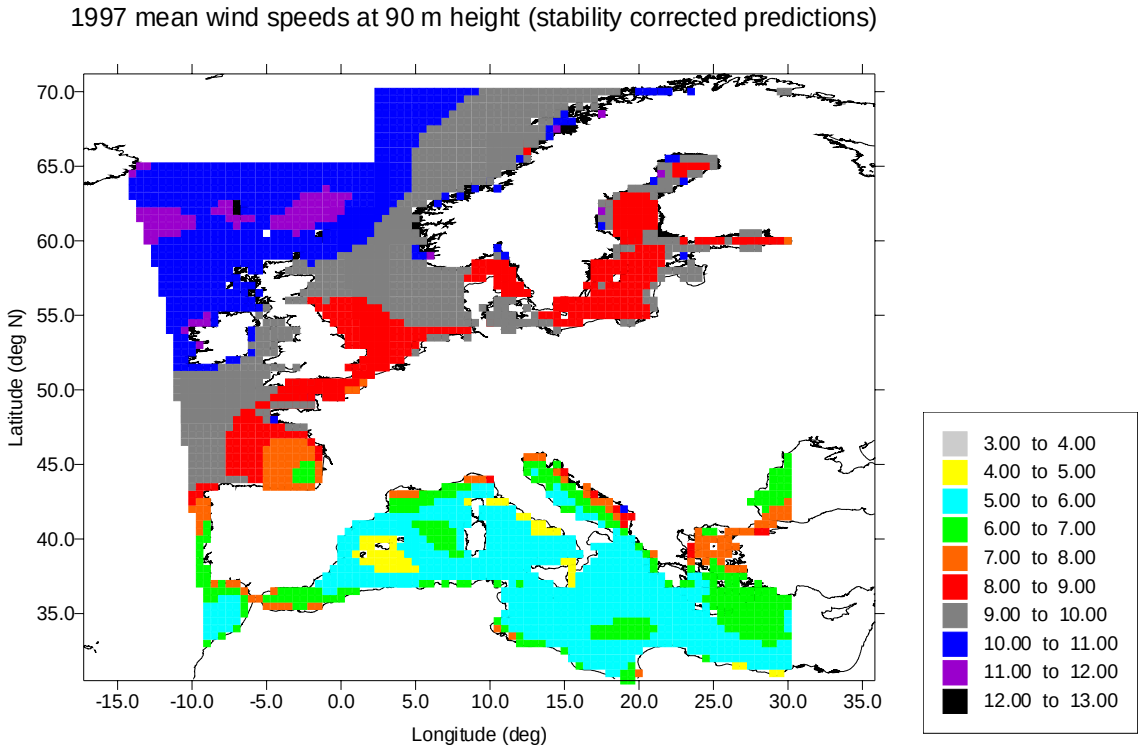

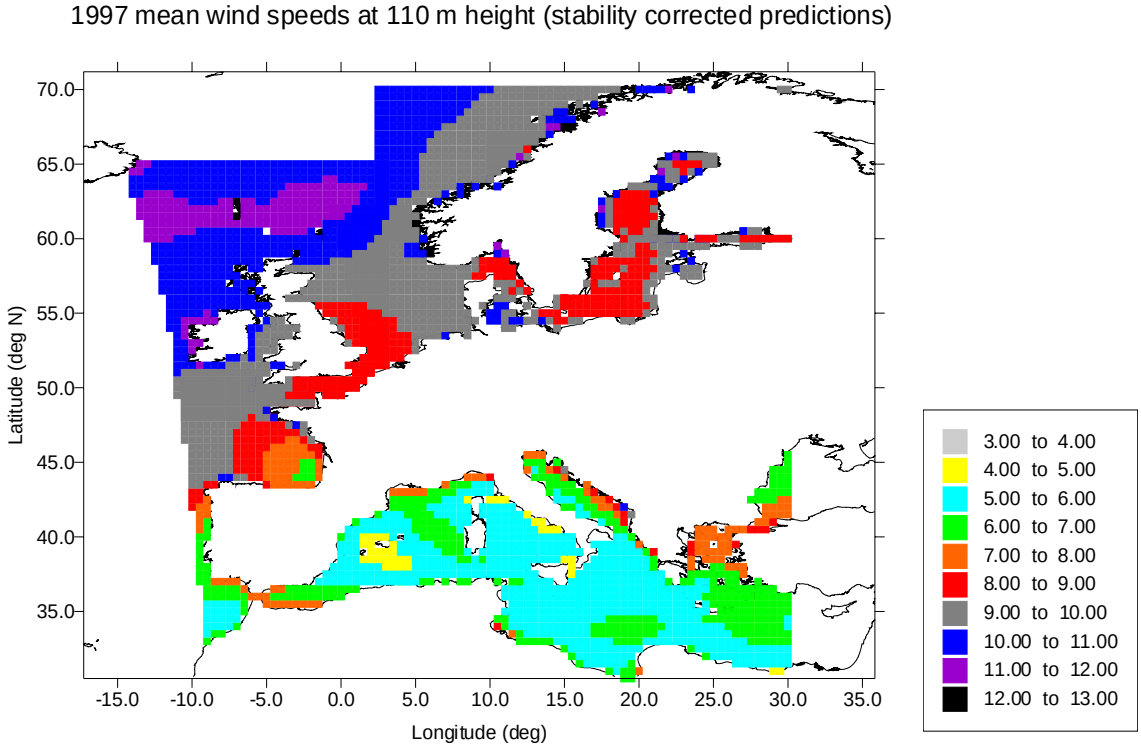

Figure 5-7. (continued).

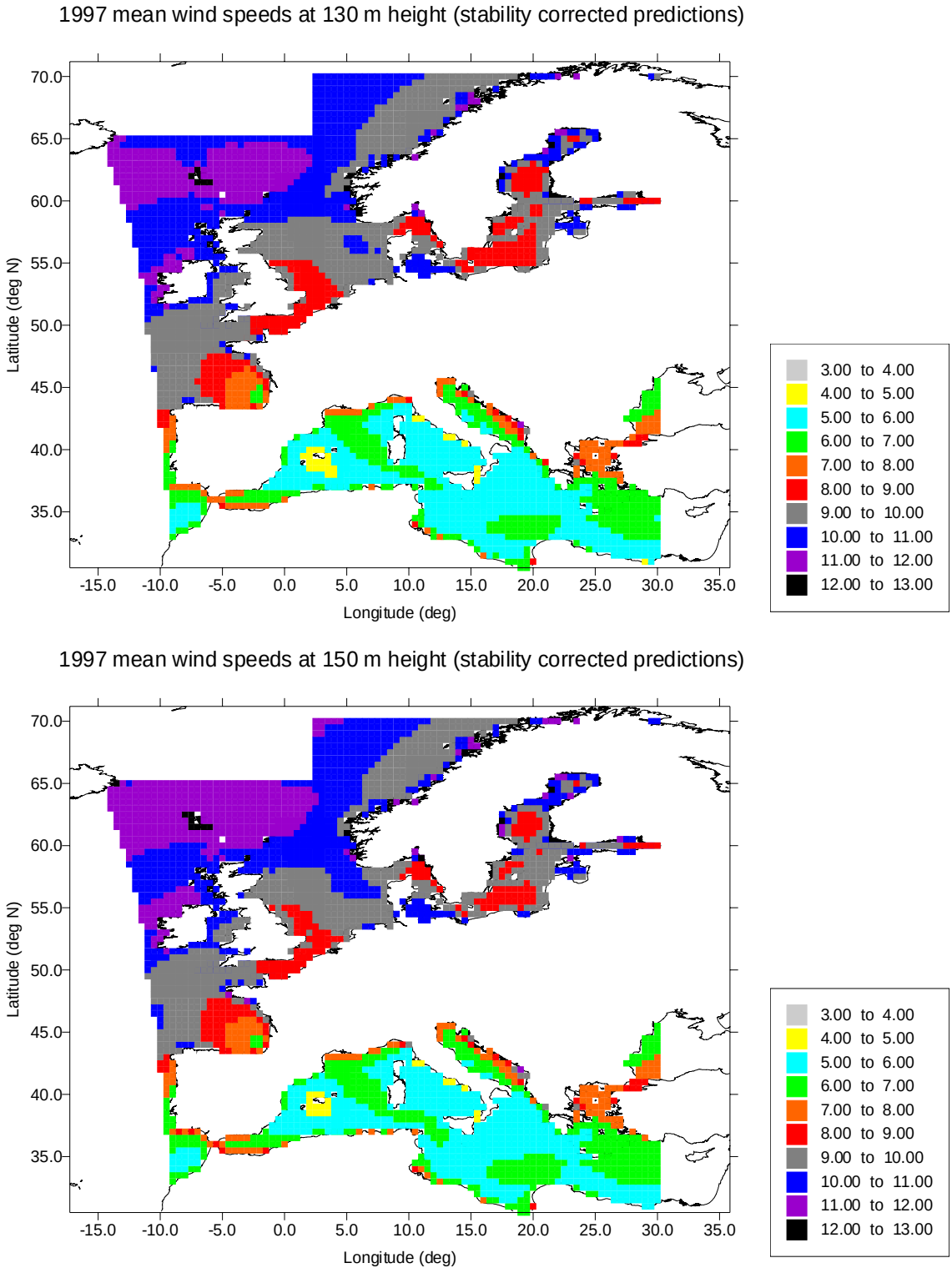

Figure 5-7. (continued).

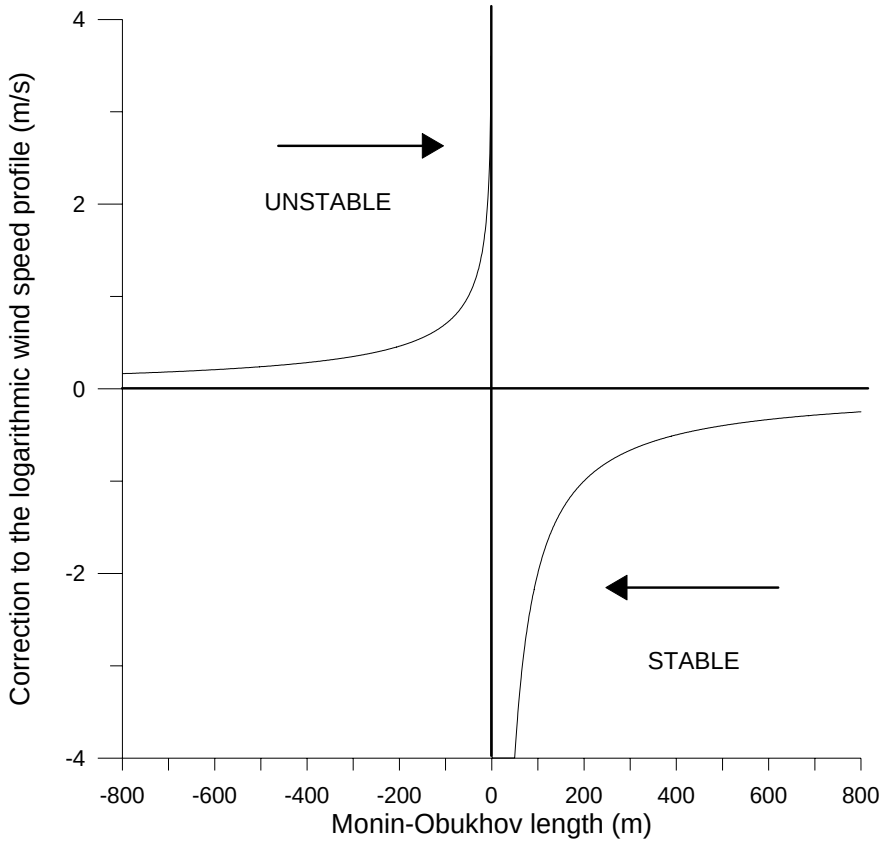

Figure 5-8. Corrections to the wind profile at 40 m based on the Monin-Obukhov length.

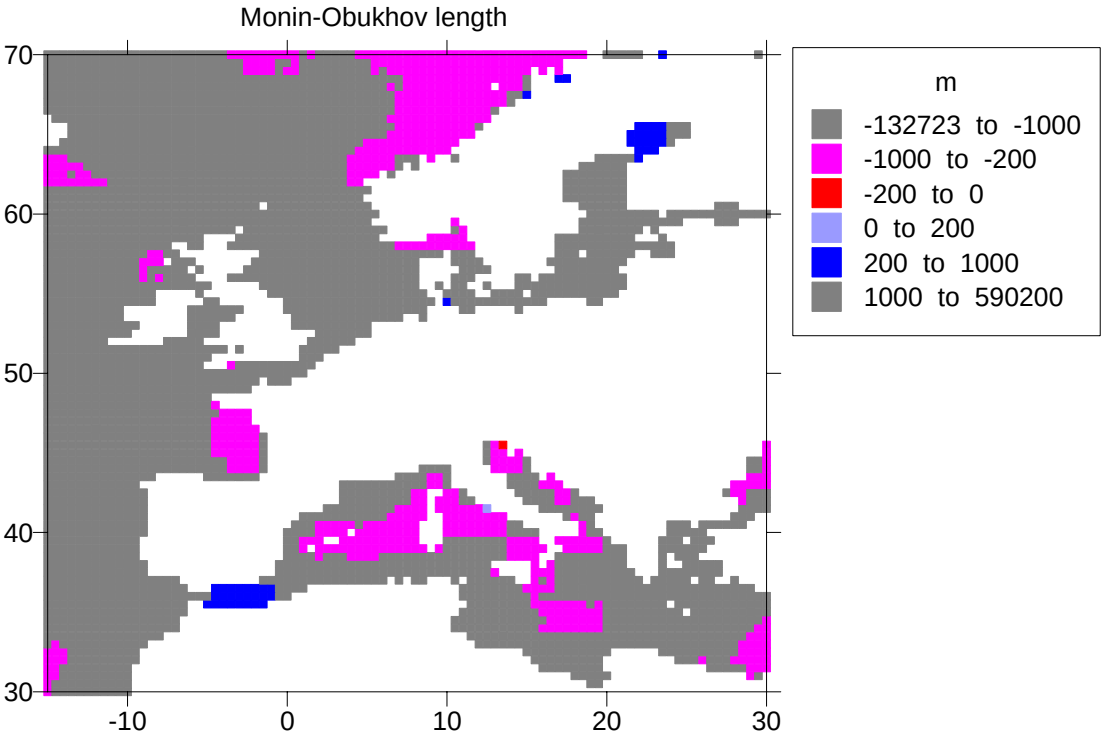

Figure 5-9. CDM calculations of the mean Monin-Obukhov length.

5.2.3 The role of variable surface roughness and tidal range

Variable roughness offshore impacts air-sea exchange and has been extensively studied. If a constant value for roughness of 0.001 to 0.0002 m is not used, the most commonly utilised is the Charnock formula (Charnock, 1955) which estimates roughness based on the friction velocity:

$$z_0 = a\frac{u_*^2}{g} \tag{5.6}$$

where g is acceleration due to gravity and
a is a constant.

As described in (Donelan *et al.*, 1993) the value of a is not constant but has been found to vary from about 0.011 (Smith, 1988) in well-developed seas to 0.018 in coastal areas (Garratt, 1977). Observations and modelling studies (e.g. (Kitaigorodsky and Zislavsky, 1974), (Geernaert *et al.*, 1986), (Nordeng, 1991)) have suggested that a is fetch-wind speed dependent (where fetch is defined as the upwind distance to the coastline), and various formulations for the fetch or wave height dependence of roughness have been proposed e.g. (Johnson *et al.*, 1997).

Discussions of the impact of roughness length on offshore wind resources have mainly focussed on two points:

1) the roughness dependence on wind speed impacts wind speed profiles at higher wind speeds
2) these effects are most important at relatively short fetches

Results of a modelling study by Frank et al. (2000) suggest that using the simplest approach (constant roughness of 0.2 mm as used in WAsP) compared with either Charnock (wind speed dependent roughness) or a fetch dependent roughness gave a relatively small difference in the predicted wind speed (less than 0.5%) even at short fetch distances of 5 km. Frank et al. (2000) suggested that thermal stratification has a much greater impact on offshore wind resources than changes in roughness.

This point can be illustrated by the following. If stability is close to neutral and conditions are in equilibrium then a logarithmic profile is assumed to fit the observed wind speed profile. If wind speed at 10 m height is known then the variation in the effect of roughness can be determined by using the logarithmic wind speed profile. Wind speeds are assumed to lie in the range 5-25 m/s (normal operating range of a wind turbine).

The following observations can be made based on results in Frank et al. (2000):

1. For fetches between 15 and 60 km differences in roughness length are only predicted at wind speeds higher than 12 m/s. In the range of wind speeds 12-25 m/s the maximum difference in roughness between 15 and 60 km fetch is 0.01 m at 15 km and 0.003 m at 60 km. As shown in Table 5-1, this gives a maximum difference of 2.8% in the log-predicted wind speed at 50 m from a 25 m/s wind speed at 10 m height. At more moderate wind speeds (e.g. 15 m/s) the difference in roughness length is 0.0009 m at 60 km fetch to 0.001 m at 15 km. This gives a difference of less than 0.2% in predicted wind speed at 50 m height.
2. Differences in roughness length are larger between open sea (here 60 km fetch) and coastal areas (2 km fetch). At 25 m/s the roughness lengths at 2 km fetch and 60 km fetch are 0.03m and 0.003m. This gives the maximum possible difference in predicted wind speed at 50 m height of 8%. At more moderate wind speeds of 15 m/s the difference in roughness length is 0.0009 m at 60 km fetch to 0.005 m at 2 km fetch. This gives a difference of 3.2% in predicted wind speed at 50 m height.
3. At lower wind speeds the difference in roughness length and hence in predicted wind speed are smaller.

A further point should be made which has not yet been addressed in great detail – the impact of swell or tidal range on predicted wind speed. The reason that tidal range is important is that wind speed extrapolation with height is typically made to a fixed reference height. If the increase in wind speed between the reference height (e.g. 10 m) and a greater height (e.g. 50 m) is based on the logarithmic profile, then the wind speed factor used varies if the distance to the surface varies. The natural logarithm of the reference height is more strongly impacted by the change height of the surface.

Figure 5-10 illustrates this principle for a tidal range of 2 m for three different wind speed scenarios; fixed, typical ‘diurnal’ profile and a ‘cosine’ profile. Note that each has a mean wind speed of 7m/s. While the predicted wind speed varies for the tidal range shown by hour, the differences in the average wind speed over this period is less than 0.1 m/s. As the tidal range increases, the impact of the changing height increase to about 0.2 m/s for a tidal range of 4 m but remains less than 0.3 m/s for wind speeds up to 25 m/s. Thus if the wind profile is close to logarithmic and the tidal range less than 4m, the impact on the predicted wind speed profile up to 50 m height is

expected to be negligible. However, if the height used to predict the wind speed profile is below 10 m from mean sea level the impact will be larger.

Given the relatively small impact of roughness changes on mean wind speed profiles in comparison with other error sources and the difficulty of developing an algorithm combined with obtaining data on wave height and wave age, the Charnock formula is used within the CDM. A constant roughness of 0.0002 m is used in WAsP but the use of two different algorithms is not expected to cause very large differences in the predicted wind speed profiles.

Table 5-1. Predicted wind speed using logarithmic wind speed profile and different roughnesses

		Roughness length (m)									
Wind speed (m/s)	Height (m)	0.03	0.02	0.01	0.005	0.003	0.002	0.001	0.0009	0.0002	0.00002
5	10	5.00	5.00	5.00	5.00	5.00	5.00	5.00	5.00	5.00	5.00
	50	6.39	6.29	6.16	6.06	5.99	5.94	5.87	5.86	5.74	5.61
	100	6.98	6.85	6.67	6.51	6.42	6.35	6.25	6.24	6.06	5.88
7	10	7.00	7.00	7.00	7.00	7.00	7.00	7.00	7.00	7.00	7.00
	50	8.94	8.81	8.63	8.48	8.39	8.32	8.22	8.21	8.04	7.86
	100	9.77	9.59	9.33	9.12	8.99	8.89	8.75	8.73	8.49	8.23
9	10	9.00	9.00	9.00	9.00	9.00	9.00	9.00	9.00	9.00	9.00
	50	11.49	11.33	11.10	10.91	10.79	10.70	10.57	10.55	10.34	10.10
	100	12.57	12.33	12.00	11.73	11.55	11.43	11.25	11.22	10.92	10.58
11	10	11.00	11.00	11.00	11.00	11.00	11.00	11.00	11.00	11.00	11.00
	50	14.05	13.85	13.56	13.33	13.18	13.08	12.92	12.90	12.64	12.35
	100	15.36	15.08	14.67	14.33	14.12	13.97	13.75	13.72	13.34	12.93
13	10	13.00	13.00	13.00	13.00	13.00	13.00	13.00	13.00	13.00	13.00
	50	16.60	16.37	16.03	15.75	15.58	15.46	15.27	15.25	14.93	14.59
	100	18.15	17.82	17.33	16.94	16.69	16.51	16.25	16.21	15.77	15.28
15	10	15.00	15.00	15.00	15.00	15.00	15.00	15.00	15.00	15.00	15.00
	50	19.16	18.88	18.49	18.18	17.98	17.83	17.62	17.59	17.23	16.84
	100	20.95	20.56	20.00	19.54	19.26	19.06	18.75	18.71	18.19	17.63
17	10	17.00	17.00	17.00	17.00	17.00	17.00	17.00	17.00	17.00	17.00
	50	21.71	21.40	20.96	20.60	20.37	20.21	19.97	19.94	19.53	19.09
	100	23.74	23.30	22.67	22.15	21.83	21.60	21.25	21.20	20.62	19.98
19	10	19.00	19.00	19.00	19.00	19.00	19.00	19.00	19.00	19.00	19.00
	50	24.26	23.92	23.43	23.02	22.77	22.59	22.32	22.28	21.83	21.33
	100	26.53	26.04	25.33	24.76	24.39	24.14	23.75	23.70	23.04	22.33
25	10	25.00	25.00	25.00	25.00	25.00	25.00	25.00	25.00	25.00	25.00
	50	31.93	31.47	30.82	30.29	29.96	29.72	29.37	29.32	28.72	28.07
	100	34.91	34.26	33.33	32.57	32.10	31.76	31.25	31.18	30.32	29.39

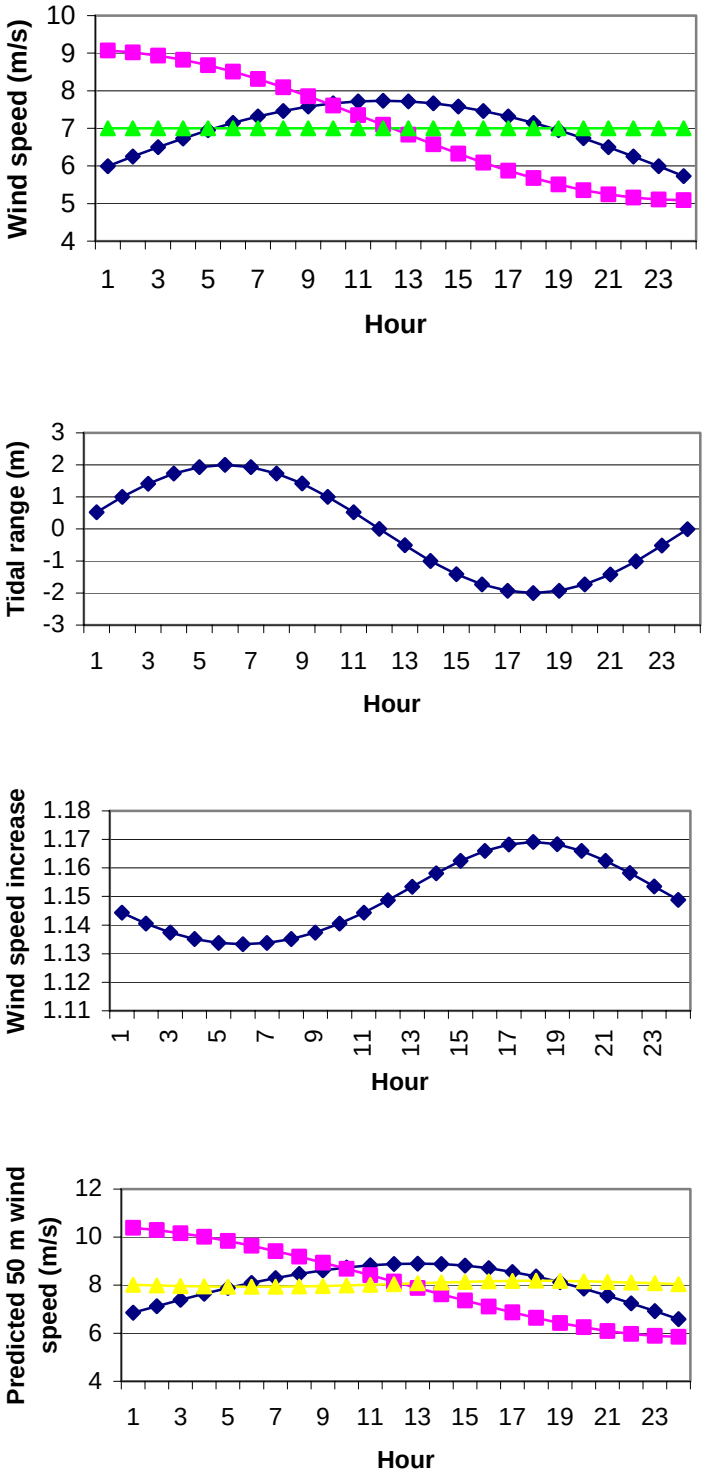

Figure 5-10: Impact of tidal range on predicted wind speed. Top: Wind speed scenario Next: Tidal range. Next: Wind speed increase between 10 m and 50 m height Bottom: Predicted wind speed at 50 m height. (from Barthelmie, 2000).

5.2.4 The impact of stability on offshore flow

Modification of the flow in the coastal zone as a result of the discontinuity in stability and roughness has profound implications for the wind speed distribution and hence for offshore wind energy production. [*Pryor and Barthelmie, 1998*] found that with offshore flow at 1.2-1.7 km from the coast the flow to the new surface conditions had propagated vertically to at least 20 m height. However, the form of the wind speed distributions above 20 m height were not statistically different at the sea masts indicating that flow at this height had not significantly changed as a result of the modified surface conditions. [*Pryor and Barthelmie, 1999*] extend this analysis further to examine fetch dependence of flow modification using data from Gedser land mast (located on the tip of a north-south oriented island) and the Rødsand mast (located approximately 11 km offshore to the west). Using conditional sampling the data from Rødsand and Gedser were classified based on stability (as determined from application of the [*Beljaars et al., 1989*] routines) and fetch characteristics (i.e. distance to the coast-line along the prevailing wind direction). Figure 5-11 shows the wind speed distributions from the two masts at 10 and 50 m height sampled by fetch and stability class (for over land flow to the Gedser mast, and over sea flow to the Rødsand mast). As shown, acceleration of the flow due to the lower roughness of the sea surface is most marked at 10 m height under all stability conditions and is much less pronounced at 50 m.

These distributions have been quantitatively compared using two standard statistical tests:

- The Wilcoxon matched-pairs signed ranks test (which tests the equality of the magnitude of observations in two series)
- The Kolmogorov-Smirnov equality of distributions test (which tests whether the form of two distributions is similar).

As expected, wind speed distributions at all heights and in all stability classes indicated higher wind speeds at the sea mast (i.e. significant Wilcoxon matched pair results). The results also indicate that except at the 50 m height the wind speed distributions exhibit a different form at the Gedser and Rødsand masts. It is hypothesised that this is due to a change in momentum exchange with the surface which causes a modification of the wind speed profile. At 50 m height, however, the adjustment to the modified surface fluxes has not significantly altered the form of the wind speed distribution even after a fetch of over 20 km. This suggests that at this height the flow characteristics are still heavily influenced by the land surface over which the wind had previously blown. The exception to this result is found under stable conditions with short fetch. This anomaly is the subject of further analysis and can not currently be explained. Both sets of analysis suggest that the width of the coastal zone (the offshore area which is affected by the presence of land) is strongly dependent on the height examined and the prevailing stability conditions. Hence the CDM utilises a coastal band of 50 km. If the grid point is less than 50 km from the coast the CDM calculates equilibrium on- and offshore wind speed profiles and the IBL height according to stability conditions and then predicts the wind speed profile at the given distance.

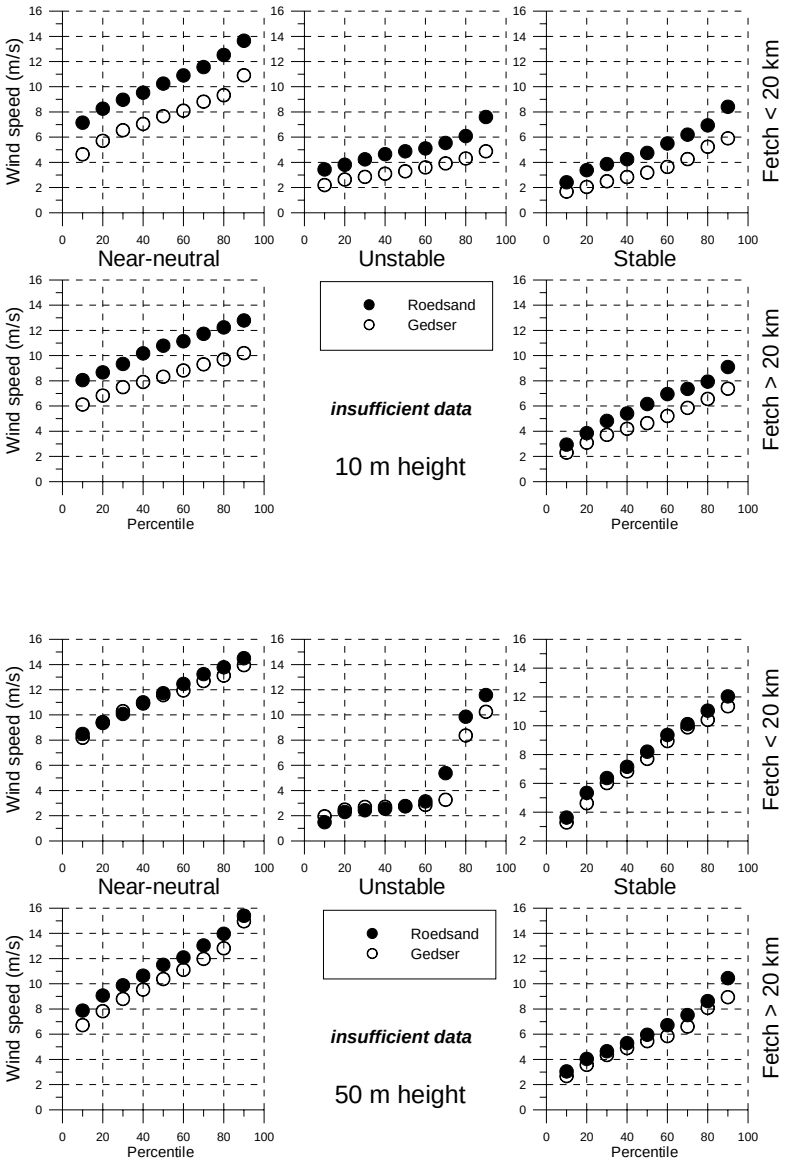

Figure 5-11. Wind speed distributions from Gedser land mast and Rødsand sea mast at 10 m and 50 m for flow over land to the Gedser mast and over sea (with varying fetch) at the Rødsand mast under different stability conditions. Fetch refers to the oversea fetch distance to the Rødsand mast.

5.3 Integrating the CDM and WAsP for the POWER project

5.3.1 Comparison of predictions based on geostrophic wind speeds

In this section both WAsP and the CDM are initialised with geostrophic wind speeds for the period 1985-97. Results from these models are denoted here as GEO-WAsP and GEO-CDM, respectively. Predicted near-surface wind speeds are compared to evaluate the differences produced by the different algorithms as discussed in section 5.2.1.

5.3.1.1 Comparing the neutral GEO-CDM with GEO-WAsP

Major differences are observed between the GEO-WAsP and neutral GEO-CDM predictions which are unexpected in far offshore areas. Differences in wind speed predictions are expected close to the coast where topography, stability and the IBL height are important. However, in near-neutral conditions, it is anticipated that these differences are negligible beyond 10 km from the coast line. The most likely cause of differences in the wind speeds shown in Figure 5-12 is the stable correction to the wind speed profile above the sea which WAsP applies. A further possibility which should be investigated is that the iteration procedure using the Charnock relationship in the GEO-CDM is producing a friction velocity which is too low.

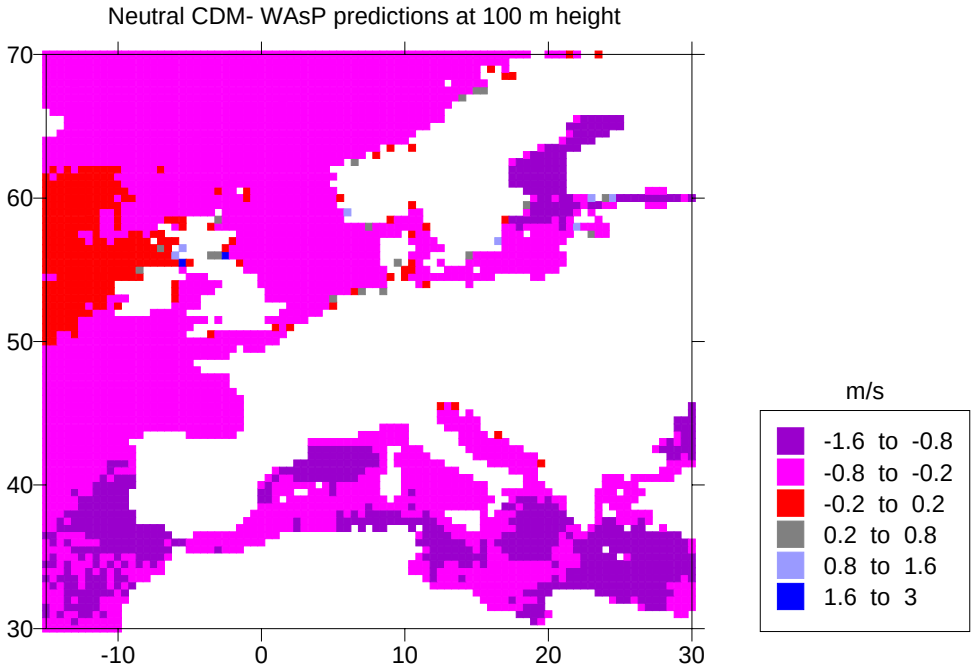

Figure 5-12. Differences in wind speed predicted at 100 m height between the neutral GEO-CDM and GEO-WAsP models (mean for the period 1985-97)

5.3.1.2 Comparing the stability corrected GEO-CDM with GEO-WAsP

Figure 5-13 shows GEO-WAsP predicted wind speeds at 10 m height, GEO-CDM predicted wind speeds at 10 m height, the difference in each grid square and the air-sea temperature difference. As illustrated differences in the wind speed prediction do not appear to be related to the pattern of air-sea temperature differences. Figure 5-14 shows the GEO-CDM stability correction at 10 m. The stability correction is likely to be most important in areas with relatively low wind speeds since higher wind speeds will tend to increase the value of the Monin-Obukhov length. Hence the stability correction is mainly large in Mediterranean. Relatively large stability corrections driven by large air-sea temperature differences are also present along the north Norwegian coast and in the north Baltic. The atmosphere over the Baltic is known to be slightly stable on average (implying that air temperatures are typically higher than sea surface temperatures). However, differences in the north Norwegian Sea were not expected.

Figure 5-15 shows the difference in wind speeds at 100m between the wind speeds predicted from the stability corrected GEO-CDM and GEO-WAsP models. Biggest differences are found in the Mediterranean region. As shown in Figure 5-16 at 10m height, stability corrections predicted by in the GEO-CDM are only important in coastal regions.

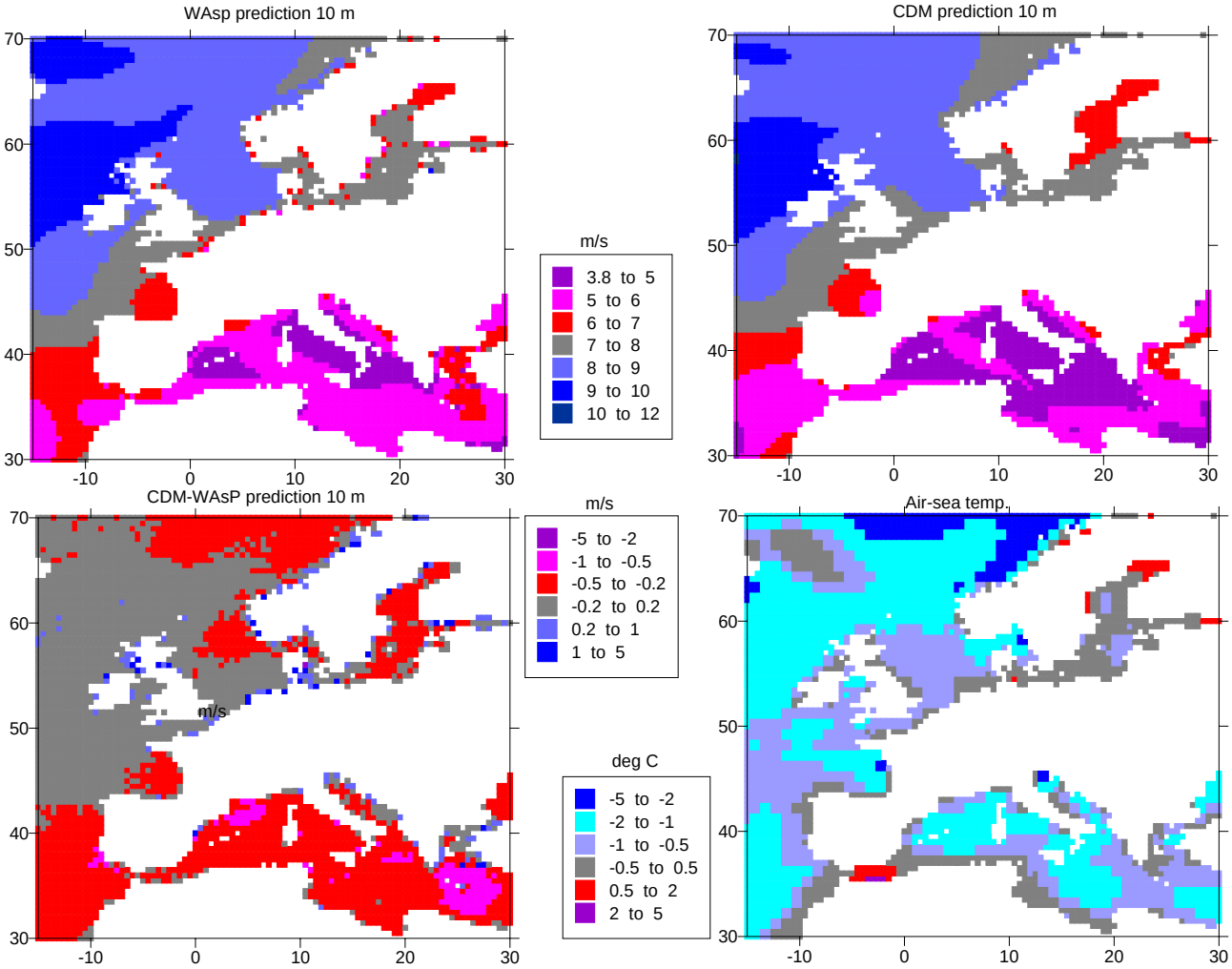

Figure 5-13. GEO-WAsP predicted wind speeds at 10 m height, GEO-CDM predicted wind speeds at 10 m height, the difference in each grid square and the air-sea temperature difference (mean for the period 1985-97).

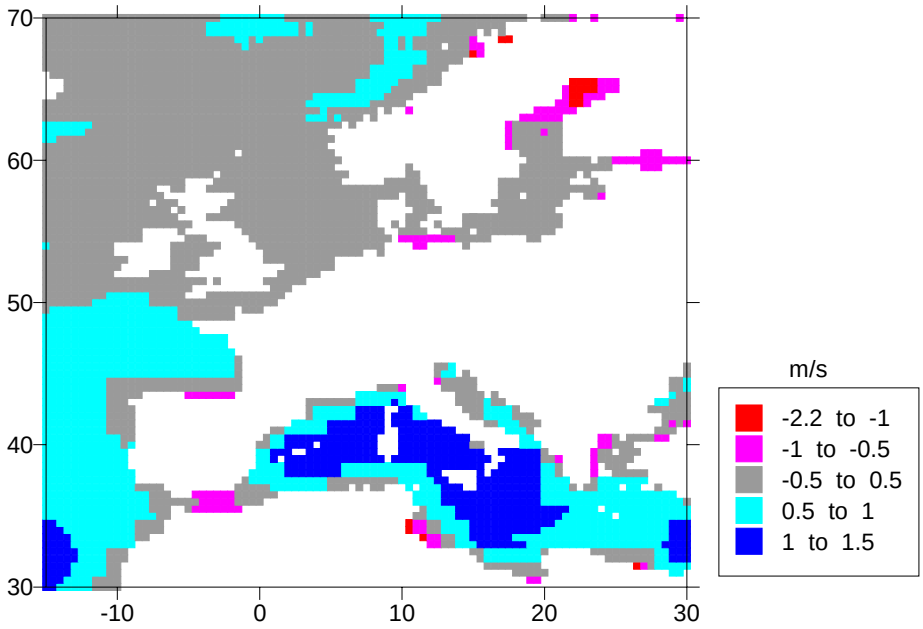

Figure 5-14. GEO-CDM calculated stability correction at 10 m (mean for the period 1985-97).

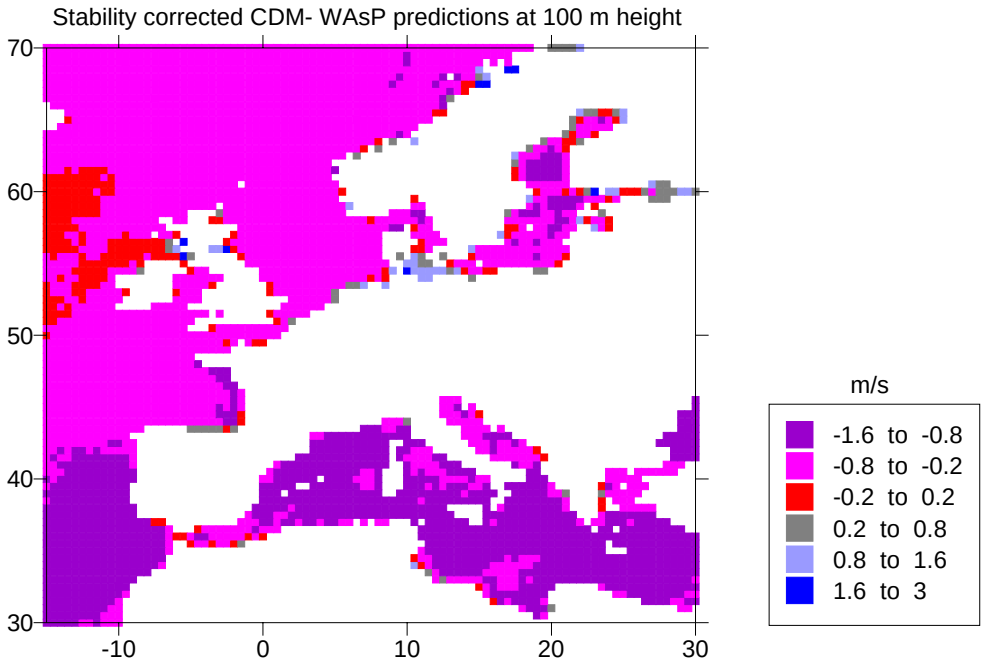

Figure 5-15. Differences in wind speed predicted at 100 m height between the stability corrected GEO-CDM and GEO-WAsP models (mean for the period 1985-97)

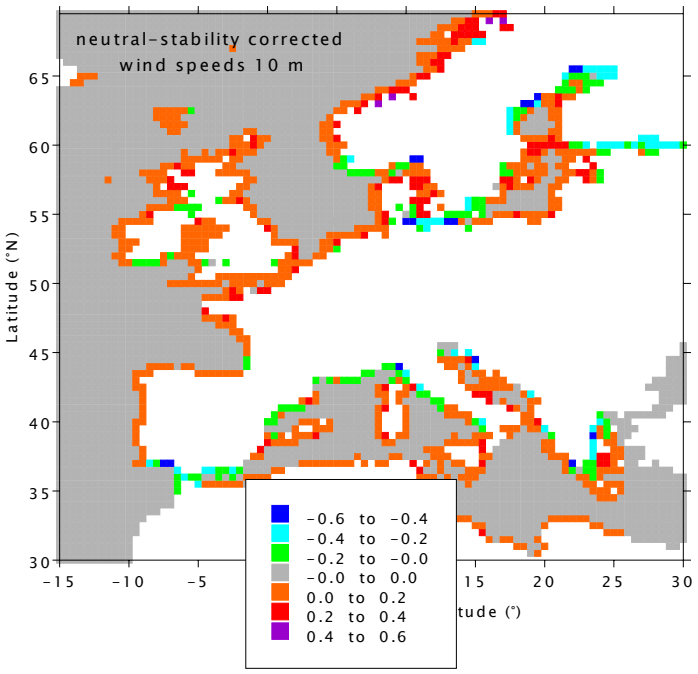

Figure 5-16. Differences in wind speed predicted at 10 m height between the stability corrected GEO-CDM and neutral GEO-CDM formulations (mean for the period 1985-97).

5.3.2 Applying the CDM to WAsP predicted wind speeds

5.3.2.1 General approach

In order to correct WAsP wind speeds for observation-specific stability (rather than the general stability correction applied in the typical application of WAsP) the general stability correction has to be removed from the WAsP predictions. Following this, the stability correction is calculated as in Barthelmie (1999) (based on the Monin-Obukhov length determined from grid-specific wind speeds and air and sea temperatures) and applied to each observation. It should be noted that neither the CDM nor WAsP account for large scale thermal flows such as the sea breeze and low level jets.

Both the Coastal Discontinuity Model (CDM) and the Wind Analysis and Application Programme (WAsP) (Mortensen *et al.*, 1993) can be initialised with geostrophic wind speeds and used to predict near-surface winds as described above. The main differences in the predicted wind fields stem from:

- *The transformation from geostrophic to near-surface winds.*

  In both models the geostrophic drag lag is used to estimate the friction velocity from the geostrophic wind speed U_g which can be used to predict near-surface winds. The same values for the constants A and B are used where A=1.8 and B=4.5.

$$U_g = \frac{u_*}{k}\sqrt{\left(\left(\ln\left(\frac{u_*}{fz_0}\right) - A\right)^2 + B^2\right)}$$

  Here the CDM uses an iterative procedure since the value of the roughness length z_0 over sea is determined according to the Charnock equation (Charnock, 1955) (i.e. varies with wind speed) rather than the fixed value of 0.0002 m used in WAsP.

- *The calculation of the internal boundary layer height*

  Within WAsP the calculation of the internal boundary layer height, *h*, (IBL) is dependent on both the roughness and the fetch based on (Panofsky, 1973):

$$\frac{h}{z_0'}\left(\ln\frac{h}{z_0'} - 1\right) = 0.9\frac{x}{z_0'}$$

  where

  z_0' is the highest value of the two roughnesses at the discontinuity

  x is the distance to the discontinuity

  Additionally, a weighting factor is used to account for the approach to equilibrium at large distances from the discontinuity (Troen and Petersen, 1989). This decay length is 10000 m (Mortensen *et al.*, 1993).

  In practice the roughness change model is more complicated. A three layer IBL model is employed as described in (Troen and Petersen, 1989) to ensure a smooth transition of the wind speed profile over roughness changes. Here the defaults for the heights of the layers are:

  inner (lowest) layer : 0.09 *h*
  outer layer : 0.3 *h*

  An example of the WAsP predicted wind speed profiles moving away from the coast is given below (Figure 5-17). This is a prediction for a site in North Lolland moving away from the coast at distance 0 km to 9 km. As is illustrated, the majority of the wind speed adjustment close to the

surface occurs in the first 2-3 km, while the shape of the wind speed profile occurs in the first 2km. Figure 5-18 shows the same data plotted as a contour plot. The IBL height (dashed line) is estimated to reach about 100 km at 2 km from the coast. Equation (1) with $z_0^{'}$=0.1 m suggests that an IBL of 100 m at about 650 m from the coast and of 150 m at 1050 m.

Within the CDM the IBL height is calculated using:

$$h = 0.2x^{(0.78-0.33z/L)}$$

When conditions are near-neutral z/L is close to zero. Thus for comparison with WAsP an IBL of 100 m is reached after about 2500 m and of 150 m after about 4000 m. This is expected to have a significant impact on wind speed profiles in coastal areas. The reason for this difference is that WAsP uses a 'generic' roughness change formula which determines the roughness change according to the highest roughness (land) which is several orders of magnitude higher than the roughness over the sea surface.

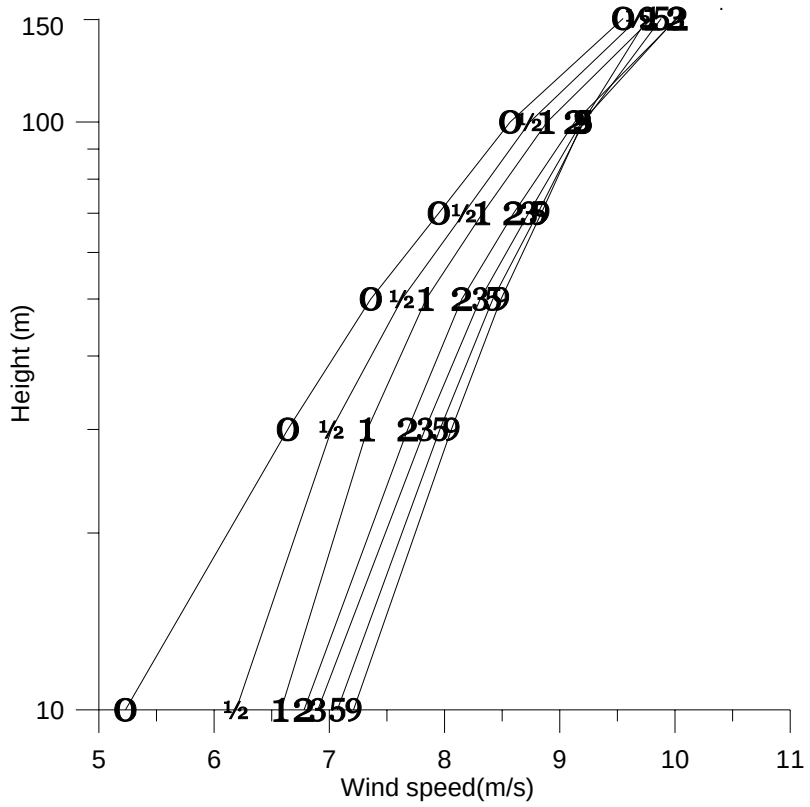

Figure 5-17. Variation of WAsP-predicted wind speed profiles moving away from the coast. Labels on the profiles indicate the distance from the coast from 0 km (coastline) to 9 km.

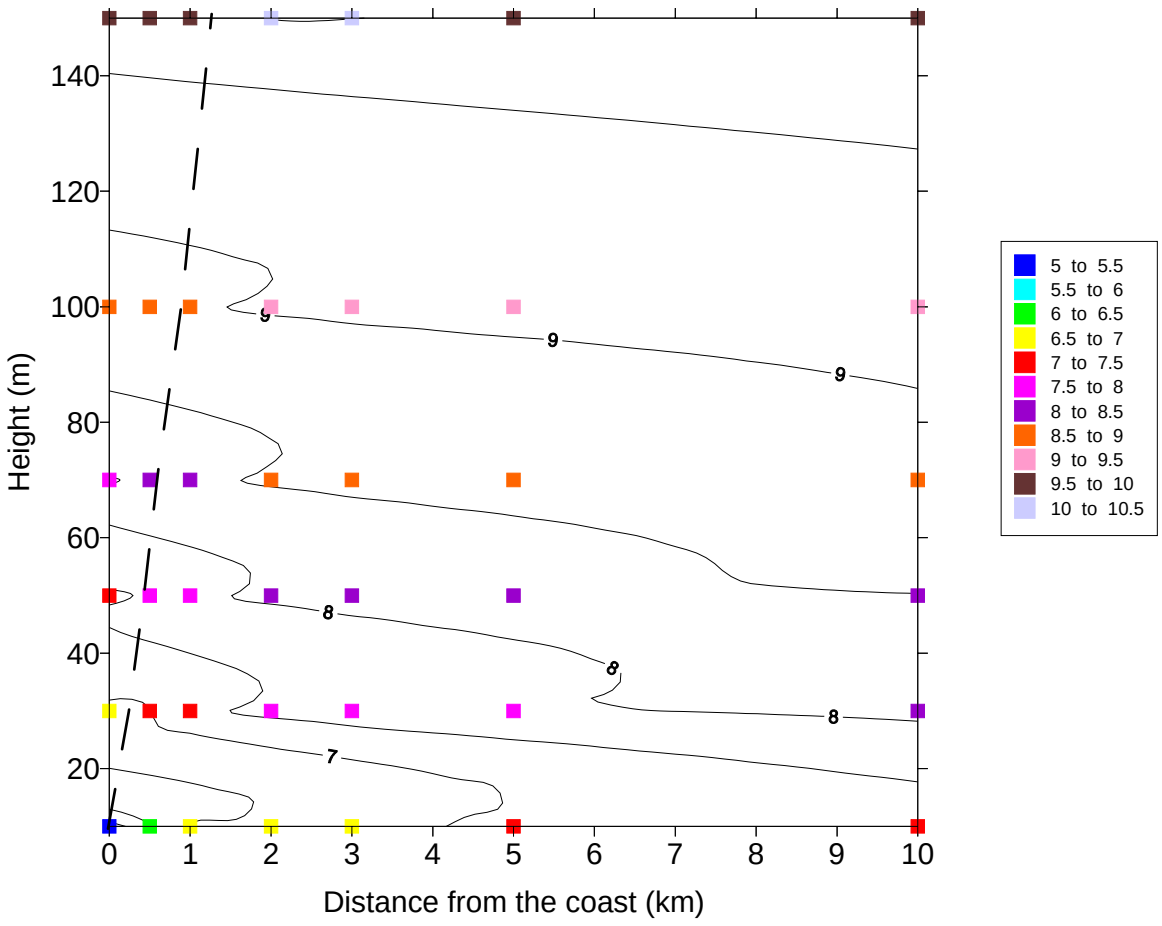

Figure 5-18. Change of wind speed profile with distance from the coast (moving offshore). The dashed line is the IBL height.

- *WAsP utilises a topographic correction*
  This maybe important in some coastal areas e.g. parts of the Mediterranean but only in the first few kilometres of the coastal zone.

- *The applied stability correction*
  WAsP applies a stability correction to the wind speed profile which reflects the underlying surface (land or sea). The difference between the correction to the profile depends on a parameter for the heat flux, its root mean square and the height to which the correction is applied (Troen and Petersen, 1989).

  Default parameters are (Mortensen *et al.*, 1993):

  1) Height of minimum correction over land 100 m (default=not used)
  2) r.m.s. of stability induced variation in wind speed over land 0.12 (default=not used)
  3) Relative increase of wind speed at height set by 1) 0.11(default=not used)
  4) Height of minimum correction sea 50 m (default=not used)
  5) r.m.s. of stability induced variation in wind speed 0.0 (default=not used)
  6) Relative increase of wind speed at height set by 4) 0.0 (default=not used)

  Thus in the general application of WAsP the stability variation is determined by the heat flux where:

  r.m.s. heat flux over land 100 Wm^{-2}
  r.m.s. heat flux over sea 30 Wm^{-2}
  Offset heat flux over land -40 Wm^{-2}
  Offset heat flux over sea 15 Wm^{-2}

Additional factors are used:

Factor in heat flux induced perturbation of u* 1.65
Form factor in heat flux distribution over land 0.6
Form factor in heat flux distribution over sea 0.6

Then corrected wind speed *u* at height *z* is:

$$u(z) = u_0(z)\left(1 + \frac{\Delta u(z_m)}{u(z_m)}\right)\left(1 - f(z)\right) + \frac{\Delta u_{*off}}{u_{*0}}$$

where:

z_m is the height of the minimum variance in wind speed
and

$$f(z) = 1 - \frac{z}{z_m}\frac{\ln(z_m / z_0)}{\ln(z / z_0)}$$

Stability correction within the CDM is carried out on an observation by observation basis. For each grid cell, a time and location specific geostrophic wind speed and direction, air temperature and sea surface temperature are used as input to the model. The friction velocity is determined assuming near-neutral conditions using the drag law and used within an iterative procedure with the temperature profile to estimate the Monin-Obukhov length (using an amended version of the methodology of (Beljaars *et al.*, 1989). This is used to correct the wind speed profile based on the Businger-Dyer flux profile relationships (see e.g. (Stull, 1988)). Then for each grid square the corrected profile is averaged for the required period.

Thus the major difference between WAsP and the CDM is that the CDM accounts for both temporal and spatial variability in stability (as reflected by the temperature profile above the sea and the wind speed) whereas WAsP applies a mean stability correction to all sea areas which is dependent on distance to the coast.

The procedure for Integrating CDM and WAsP is as follows:

1) Read WAsP output for Weibull A and k factors at each height and percentage occurrence in each sector.
2) Mean wind speed in each sector is calculated from Weibull factors:

$$U = A\Gamma\left(1 + \frac{1}{k}\right)$$

3) Mean wind speed calculated by this procedure is higher than the mean given by WAsP where:

   SUM U (SEC)=1.01*U (MEAN)

   At this point the frequency distribution of direction is available.

4) Calculate factors to correct wind speed profiles with land roughness of 0.03 m according to distance offshore and height. Two sets are required - one corrects profiles to give equilibrium on-shore wind speed profile and one gives equilibrium offshore wind speed profiles. This is done using WAsP.

5) Read in air and sea temperatures for each 1 by 1 degree grid cell. Calculate average air and sea temperatures for each grid.

6) Read in fetch distances by direction for each grid cell.

7) Merge the data sets so that each grid point has associated with it a mean wind speed profile by direction, frequency distribution by grid cell, mean air and sea temperature and a fetch distance by grid cell.

8) Use the WAsP generated wind speed profile and the air and sea temperatures to calculate an average Monin-Obukhov length by grid cell.

9) For each grid cell and each direction, use the fetch distance to interpolate between factors to correct WAsP profiles to equilibrium offshore and onshore profiles.

10) Calculate the internal boundary layer height according to fetch and stability

11) Calculate the new grid square wind speed based on the IBL height and the equilibrium offshore and onshore profiles. If the height of the wind speed to be predicted is above the IBL then the land wind speed at that height is used. If the height is below the IBL then the sea wind speed at that height is used. There is also an adjustment zone which is 10% above the IBL height and 10% below. If the height is in this region then the wind speed is extrapolated between the land and sea wind speeds, according to the log of the height. This gives a smooth transition in wind speeds over the IBL.

12) Removing the stability correction from WAsP. According to the WAsP manual there are a number of stability parameters (such as the height above ground at which the differences between stable and unstable profiles are smallest, relative increase at this height due to stability effects etc) but the default is that these are not set. However, more detailed discussion in the European Wind Atlas indicates that the treatment of stability corrections as perturbations to the neutral profile is complex. The corrections are based on average values of the heat flux where:

    rms heat flux over land=100 Wm^{-2}
    rms heat flux over sea=30 Wm^{-2}
    Offset heat flux over land=-40 Wm^{-2}
    Offset heat flux over sea=15 Wm^{-2}

The height above ground where the heat flux variations are minimum is defined by:

$$\frac{z_m}{z_0} \cong 0.002\left(\frac{G}{fz_0}\right)^{0.9}$$

where $f=2\Omega\sin\phi$ and Ω *is 7.292x10*$^{-5}$ s^{-1}

13) The direction is corrected as a linear function of the on- and offshore wind directions according to the distance from the coast

Table 5-2. Height of minimum variance for z_0=0.03m

UG/LAT	30.00	40.00	50.00	60.00	70.00
1.00	7.45	5.94	5.07	4.54	4.22
2.00	13.90	11.09	9.47	8.48	7.88
3.00	20.03	15.97	13.64	12.21	11.35
4.00	25.94	20.69	17.67	15.82	14.70
5.00	31.71	25.30	21.60	19.34	17.97
6.00	37.37	29.81	25.45	22.79	21.18
7.00	42.93	34.24	29.24	26.19	24.33
8.00	48.41	38.62	32.98	29.53	27.44
9.00	53.83	42.93	36.66	32.83	30.51
10.00	59.18	47.21	40.31	36.10	33.54
11.00	64.48	51.43	43.92	39.33	36.54
12.00	69.73	55.62	47.50	42.53	39.52
13.00	74.94	59.78	51.05	45.71	42.47
14.00	80.11	63.90	54.57	48.86	45.40
15.00	85.24	67.99	58.06	51.99	48.31
16.00	90.34	72.06	61.54	55.10	51.20
17.00	95.41	76.10	64.99	58.19	54.07
18.00	100.44	80.12	68.42	61.27	56.93
19.00	105.45	84.11	71.83	64.32	59.76
20.00	110.44	88.09	75.22	67.36	62.59
21.00	115.39	92.04	78.60	70.38	65.40
22.00	120.33	95.98	81.96	73.39	68.19
23.00	125.24	99.90	85.31	76.39	70.98
24.00	130.13	103.80	88.64	79.37	73.75
25.00	135.00	107.68	91.95	82.34	76.51

Table 5-3. Height of minimum variance for z_0=0.0002 m

UG/LAT	30.00	40.00	50.00	60.00	70.00
1.00	4.51	3.60	3.07	2.75	2.56
2.00	8.42	6.72	5.74	5.14	4.77
3.00	12.13	9.68	8.26	7.40	6.88
4.00	15.72	12.54	10.71	9.59	8.91
5.00	19.22	15.33	13.09	11.72	10.89
6.00	22.64	18.06	15.42	13.81	12.83
7.00	26.01	20.75	17.72	15.87	14.74
8.00	29.33	23.40	19.98	17.89	16.62
9.00	32.61	26.01	22.21	19.89	18.48
10.00	35.86	28.60	24.42	21.87	20.32
11.00	39.07	31.16	26.61	23.83	22.14
12.00	42.25	33.70	28.78	25.77	23.95
13.00	45.41	36.22	30.93	27.70	25.73
14.00	48.54	38.72	33.06	29.61	27.51
15.00	51.65	41.20	35.18	31.50	29.27
16.00	54.74	43.66	37.28	33.39	31.02
17.00	57.81	46.11	39.37	35.26	32.76
18.00	60.86	48.54	41.45	37.12	34.49
19.00	63.89	50.96	43.52	38.97	36.21
20.00	66.91	53.37	45.58	40.81	37.92
21.00	69.91	55.77	47.62	42.64	39.62
22.00	72.90	58.15	49.66	44.47	41.32
23.00	75.88	60.53	51.69	46.28	43.00
24.00	78.84	62.89	53.70	48.09	44.68
25.00	81.79	65.24	55.71	49.89	46.36

5.3.2.2 Results

Figure 5-19 shows results of applying the CDM to WAsP predicted wind speed profiles. Results from this model combination are denoted as WAsP-CDM in order to distinguish then from results generated using WAsP and geostrophic wind speeds (GEO-WAsP) and from results using the CDM to modify the wind speed profile from individual observations using stability correction and IBL calculations (WAsP-CDM). The WAsP-CDM gives slightly lower wind speeds in the North Atlantic due to a mean unstable correction in the CDM replacing a mean stable correction within WAsP. As shown in Figure 5-20, GEO-WAsP wind speeds are almost always higher than WASP-CDM predicted wind speeds. This is because the mean stability correction applied in offshore areas in WAsP is always positive (stable) whereas the mean stability correction calculated from the mean air-sea temperature difference is always small and sometimes negative (unstable).

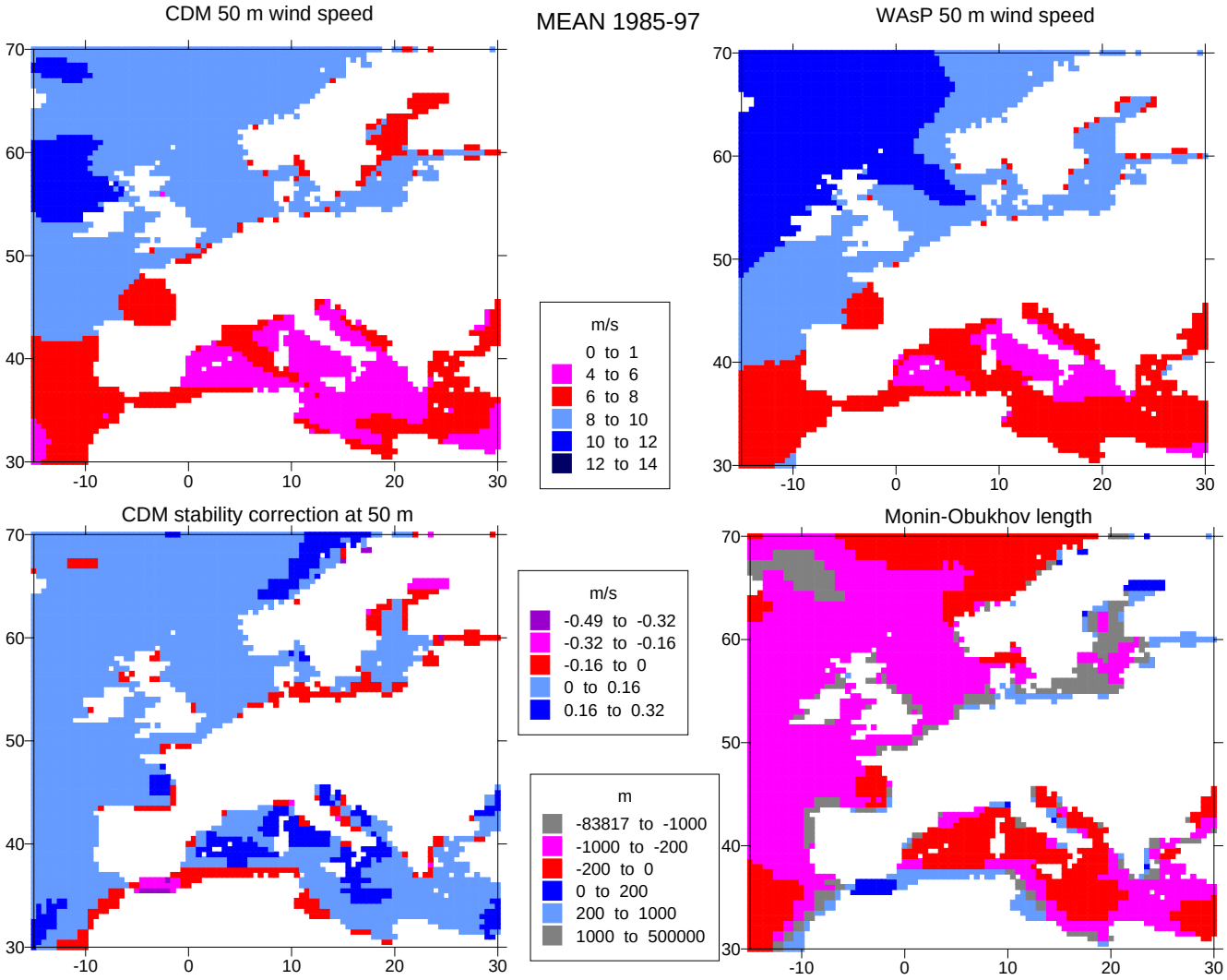

Figure 5-19. WAsP-CDM and GEO-WAsP predicted wind speeds at 50 m height for 1985-97.

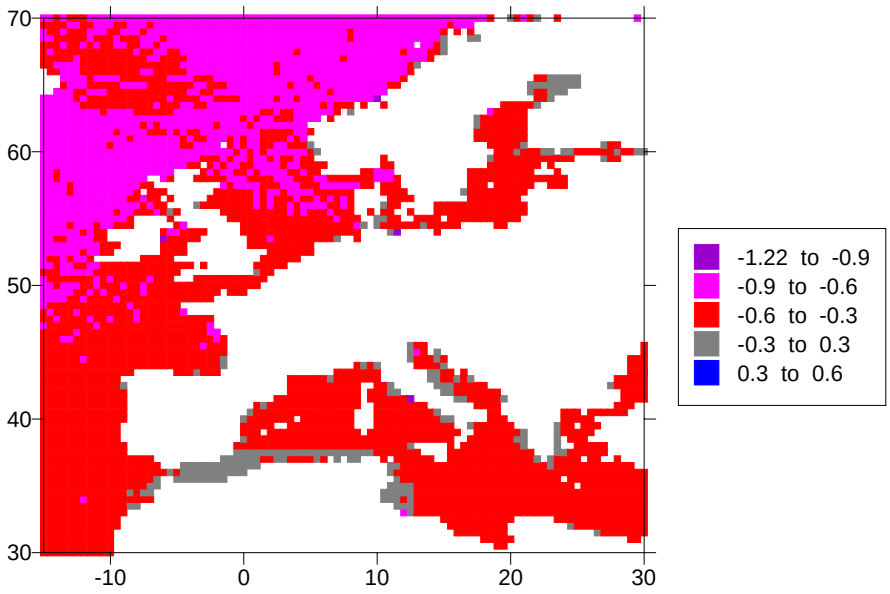

Figure 5-20 WASP-CDM minus GEO-WASP predicted wind speeds at 50 m for 1985-97 (m/s).

5.4 Validation

5.4.1 Validation of stability routines

Evaluation has been conducted as part of the POWER project using the Risø Air-Sea EXperiment (RASEX) measurements (Mahrt *et al.*, 1996) from Vindeby Sea Mast West. For details regarding site locations etc. see (Barthelmie *et al.*, 1994). The RASEX data set and the routine measurements conducted at SMW overlap for two periods: 28th April to 30th June 1994 and 17th August to 31st December 1994 giving 3645 observations for comparison. The Monin-Obukhov length calculated from direct flux measurements at 6m was compared with values based on routine measurements using a model based on flux estimation codes from Beljaars et al. (1989) which are called here Monin-Obukhov Length derived stabiLitY(MOLLY). For each half-hourly observation the Monin-Obukhov length was calculated for data from based on the corrected sea surface temperature and the absolute air temperature and wind speed at 7m height. Results of the comparison are shown in Table 5-4. There is good agreement between the frequency of different stability classes using the values of the Monin-Obukhov length calculated from fluxes measured directly and modelled using MOLLY.

Table 5-4. Comparison of frequency of stability classes at SMW based on Monin-Obukhov lengths 1) calculated using fluxes determined from data from a sonic anemometer at 6m at SMW and 2) calculated using MOLLY. Stability classes are defined according to (Van Wijk et al., 1990a) based on the Monin-Obukhov length (m).

Stability class	Monin-Obukhov length (m)	Percentage of observations	
		Direct	MOLLY
Very stable	0 < L < 200	19.5	21.1
Stable	200 < L < 1000	14.2	14.8
Near-neutral	1000 < L < -1000	9.3	9.6
Unstable	-1000 < L < -200	12.2	12.5
Very unstable	200 < L < 0	44.7	42

Since most observations offshore do not include flux measurements from which the stability parameter the Monin-Obukhov length can be calculated, this parameter is estimated using routine measurements and MOLLY. In total MOLLY has been applied at 10 sites ranging from routine synoptic coastal sites to purpose built offshore monitoring locations. MOLLY gives good results at all sites except one. At this site, (Horns Rev Fyrskib), temperature profiles were not available and a further parameterization was introduced using cloud cover to estimate radiation. This routine did not give reasonable results for this site and probably requires further modification for use in offshore areas.

The most detailed work to date has been conducted on data from the Vindeby masts (Barthelmie *et al.*, 1996a), (Barthelmie *et al.*, 1996b). (Pryor and Barthelmie, 1998) and showed that wind speed distributions at 38 m height and above are not in equilibrium with the sea surface (suggesting that they are frequently at or above the IBL). The median IBL height (two layer model) was estimated as 48 and 57 m at the two sea masts at Vindeby which are 1.2 and 1.7 km from the coast. However at heights of 20 m and below there are statistically significant differences in the wind speed distribution for on- and off-shore flow (Pryor and Barthelmie, 1998).

Using MOLLY, all sites had a mean slightly positive Monin-Obukhov length with small corrections to the logarithmic wind speed profile of between 0.1 and 0.2 m/s at heights of about 50m. This is expected since, over the course of a year, large stable corrections are typically balanced by more frequent but smaller unstable corrections to wind profiles (see also (Van Wijk *et al.*, 1990b). There was also a fetch dependence to the stability correction with the largest corrections to the wind speed profile found when offshore fetches are between 1 and 20 km from the coast and the smallest corrections (tending towards zero) when fetches exceeded about 40 km.

This suggests that for stability effects are important to about 40 km from the coast. This work is continuing to evaluate the effects of stability at seasonal and finer temporal resolution and close to the coast where the IBL is an important influence on the shape of the vertical wind speed profile and the acceleration of winds moving away from the coastline.

5.4.2 CDM modelling of SODAR derived wind speeds

As part of the POWER project, meteorological observations were made at Measurement Platform Noordvik approximately 10 km from the Dutch coast in the period January - June 2000 (see Chapter 6). A major advantage of operating a SODAR is that the SODAR observes wind speeds at greater heights than are typically monitored using a meteorological mast. Offshore masts are typically in the range 10-60 m above mean sea level whereas a SODAR should recover wind speed profiles to 100-150 m above sea level. Hub-heights of wind turbines currently being installed are in the range 60-70 m with blades of 30-40 m. Hence detailed observations of offshore wind speed profiles to 150 m are of great utility for planning offshore wind farms. However, the main objective of operating of SODAR was to provide a data set for comparison with predictions from the Coastal Discontinuity Model (CDM).

The CDM was developed to use gridded geostrophic wind speeds as input together with air and sea-surface temperatures on a 0.5 by 0.5 grid over European Seas (Barthelmie, 1999a). Since geostrophic wind speeds are not available as input to the CDM for the period of SODAR measurements, an alternative approach was required. The model uses each land-based observation to estimate geostrophic wind speed and then estimates the offshore wind profile according to fetch, estimated roughness and stability. The procedure is:

1) Use wind speed and direction from a coastal location to estimate geostrophic winds assuming that conditions are near-neutral and that the roughness length onshore is 0.03 m and offshore is 0.0002 m. Wind directions are also corrected, first transforming wind directions to geostrophic and then back at the offshore site using:

$$\sin\alpha = -Bu_* / kG$$

where α is the angle
B is a constant 4.5
u_* is the friction velocity
G is the geostrophic wind speed
k is the von Karman constant

2) Estimate friction velocity offshore based on the geostrophic wind speed using the drag law.
3) Determine the Monin-Obukhov length from observed air and water temperatures and estimated friction velocity using routines from KNMI (Beljaars *et al.*, 1989).
4) Estimate the equilibrium land and offshore wind speed profiles according to the friction velocity and roughness (either set for land or calculated using the Charnock equation (Charnock, 1955))
5) In each sector, calculate the internal boundary layer height according to fetch and stability and correct the wind speed profile.

Because wind speed profiles are not uniformly near-neutral the initial step of estimating geostrophic wind speed from land-based observations introduces a relatively large uncertainty in the estimation of geostrophic wind speeds which is propagated through the analysis. In some measurement periods the predicted wind speed at 150 m exceeded the geostrophic wind speed. In this situation, an error in the initial determination of the geostrophic wind speed was assumed and the friction velocity was reduced through an iterative procedure until all near-surface wind speeds were below that of the estimated friction velocity.

A number of assumptions have to be made. These include:

- The fetch distances to the measurement locations: Hoek van Holland (HVH), Measurement Platform Noordvik (MPN) and Ijmuiden (IJM). Site locations are given in Table 5-7. Fetch distances were estimated using WAsP (see Table 5-8 and Figure 5-21).
- Roughness of the land surface (here estimated as 0.03 m). Sector specific roughness lengths are given in Table 5-9. These were estimated using the gustiness method (Wieringa, 1976), (Wieringa, 1986).

Figure 5-21. Location of the measurement sites.

SODAR data and recovery procedure are not described in detail here since these have been reported separately (Coelingh *et al.*, 1999),(Coelingh *et al.*, 2000) – see also Chapter 6. The remaining observations required are from two sites Hoek Van Holland and IJmuiden wind speed) and the air and sea temperatures measured at MPN.

Table 5-5. Locations of the measurement sites

	Latitude	Longitude	UTM (Zone 31)		Measurement height (m)
			E (m)	N (m)	
Measurement platform Noordvik (MPN)	52°16’26” N	4°17’46”E	588299	5792090	27.6
Hoek Van Holland (HVH)	51º59’06” N	04º03’00” E	572111	5759899	15
Ijmuiden (IJM)	52º27’47” N	04º33’22” E	605593	5813215	18.5

Table 5-6. ***Fetch distances to the sites used in m. Here fetch is defined as the minimum distance to the coast.***

		HVH	MPN	IJM
1	0	>50000	>50000	17000
2	30	>50000	31800	1645
3	60	5300	12820	land
4	90	land	9730	land
5	120	land	9450	land
6	150	land	9880	land
7	180	land	13590	land
8	210	land	28480	land
9	240	>50000	>50000	19380
10	270	>50000	>50000	>50000
11	300	>50000	>50000	>50000
12	330	>50000	>50000	>50000

Table 5-7. Roughness length at IJM and HVH (m)

Sector	IJM	HVH
1	0.000193	6.18E-05
2	0.001394	7.86E-06
3	0.000908	0.000224
4	0.00066	0.001284
5	0.003108	0.000151
6	0.000538	0.000305
7	2.21E-05	0.000379
8	1.28E-06	0.001632
9	1.12E-06	0.003098
10	5.1E-06	0.000188
11	4.9E-05	7.67E-05
12	0.000108	9.62E-05

The CDM is implemented using observations from HVH to estimate geostrophic wind speeds. Using all observations during the period 24 February -16 June 2000 the observed wind speed at 15 m height is 6.62 m/s and the direction is predominately south-westerly (Figure 5-22).

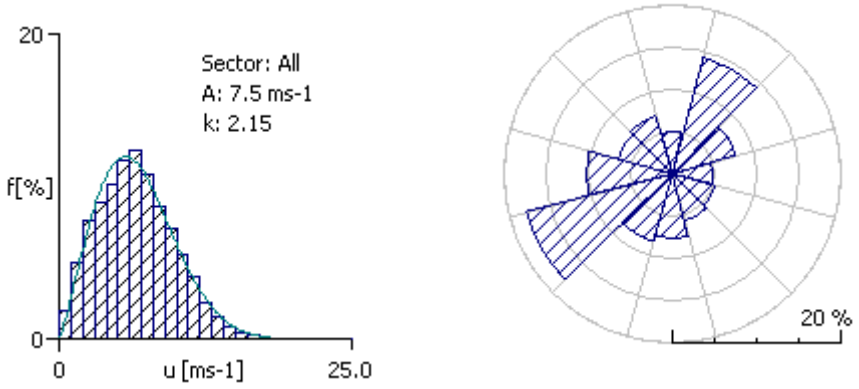

Figure 5-22. Wind speed distribution and wind rose from HVH.

Geostrophic wind speed is calculated as 9.71 m/s over the same period with a stronger westerly component in the direction (Figure 5-23).

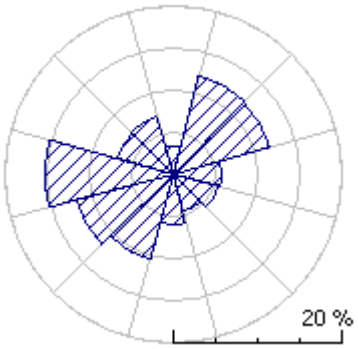

Figure 5-23. Wind rose of calculated geostrophic wind speeds.

Mean sea surface temperature (from MPN) over the same period is 9.6°C and mean air temperature is 10.1°C indicating that conditions should be slightly stable on average. Figure 5-24 shows the variation of air and sea temperature and the calculated Monin-Obukhov length over the whole period. At the

beginning of the measurement period, conditions are mainly stable whereas at the end of the period more unstable conditions are indicated.

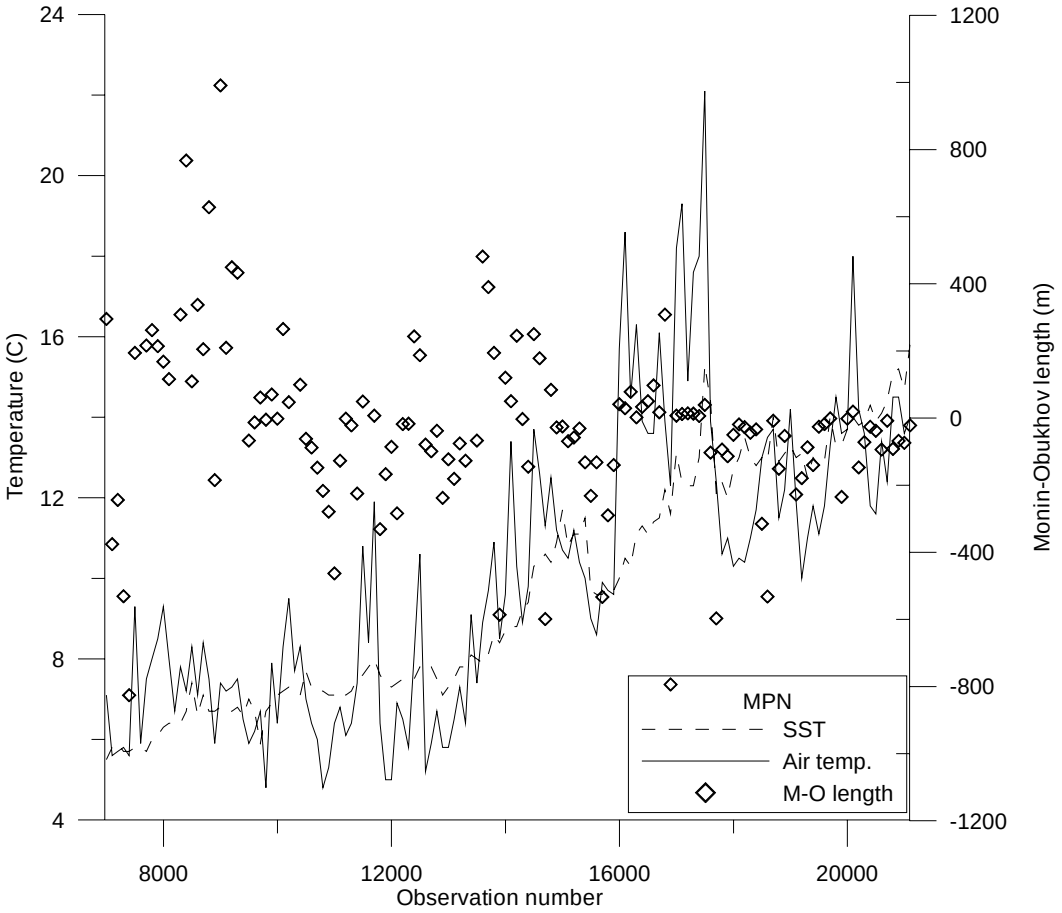

Figure 5-24. Observed air and sea surface temperature (degrees c) at MPN and estimated Monin-Obukhov length from 24 February to June 15 2000.

Figure 5-25 shows the mean wind speed profile observed by the SODAR and the predicted wind speed profile from the CDM. The observations are limited to those periods in which the SODAR collected data at all heights between 20 and 90 m. In the Figures shown below 15 m is added to the SODAR wind speed height to account for the height of the platform. Wind speeds below 55 m are excluded to the distortion of the profile by the measurement platform itself. Predictions were then made for coincident data observations excluding periods with rain. Over-prediction of wind speeds is to be expected due to the procedure used to estimate geostrophic wind speeds. However, the CDM indicates a near-neutral wind speed profile unaffected by the internal boundary layer while the SODAR observations suggest greater wind shear due either to higher roughness or to stability. Note that mean wind speeds above 90m (115 m above sea level) are included although there may be relatively few observations. Under-prediction of wind speed may be a result of predicting wind speeds for the grid square in which MPN lies rather than using actual fetch distances in each sector. In order to examine the impact of fetch, further calculations were conducted by sector (Figure 5-26), again restricting both observed and predicted wind speeds to periods of coincident observations. This reduces the number of observations in each sector. Comparing CDM predicted and SODAR observed wind speed profiles between 55 and 115 m there is considerable variability by sector. The CDM gives good predictions in Sector 1, over-predicts wind speeds in Sectors 3, 4, 5,6 and 7, under-predicts in Sectors 9,10, 11 and 12. In Sectors 2 and 8, the SODAR indicates a profile which is disrupted by thermal structures - possibly a low internal boundary layer. This distribution of over - and under- prediction by sector may indicate a problem with using HVH observations to estimate the geostrophic wind speed. Geostrophic wind speeds from HVH observations with land fetch may be overestimated due to the relatively high friction velocity while those from the sea fetch maybe underestimated due to the low friction velocity over sea. However, one feature which is not solely determined by the geostrophic wind speed is the

wind shear. The observed SODAR wind shear is greater than the CDM predictions in all sectors except 1,3 and 4. This indicates either a much higher roughness than is predicted by the CDM using the Charnock equation, or a greater thermal contribution. This is also suggested by over-prediction of the mast wind speed in these sectors. The second factor is investigated by comparing observed and predicted wind speed profiles in different stability groups.

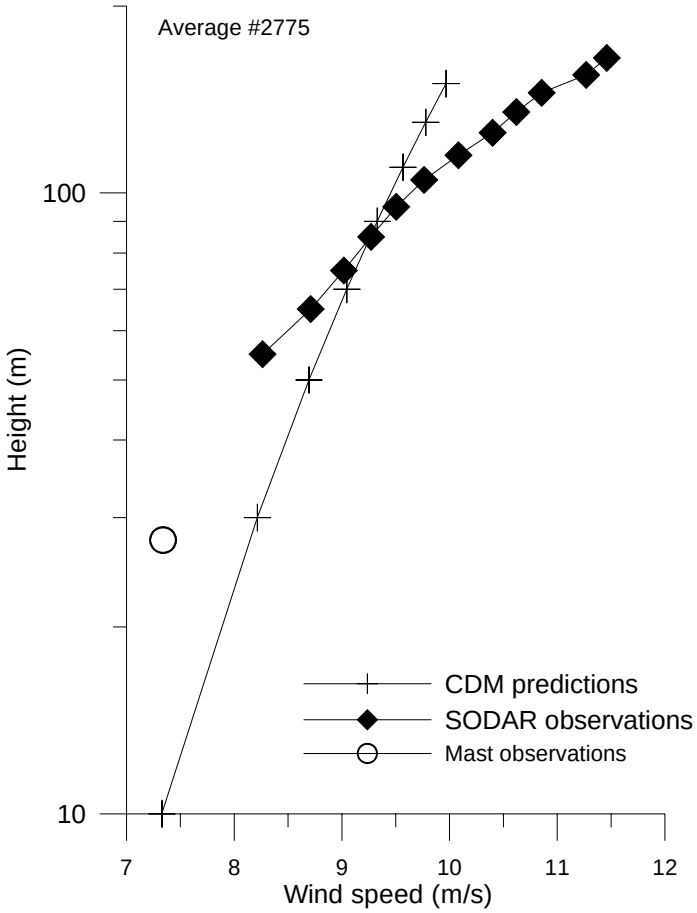

Figure 5-25. Mean wind speed profiles at MPN from the SODAR and predicted by the CDM.

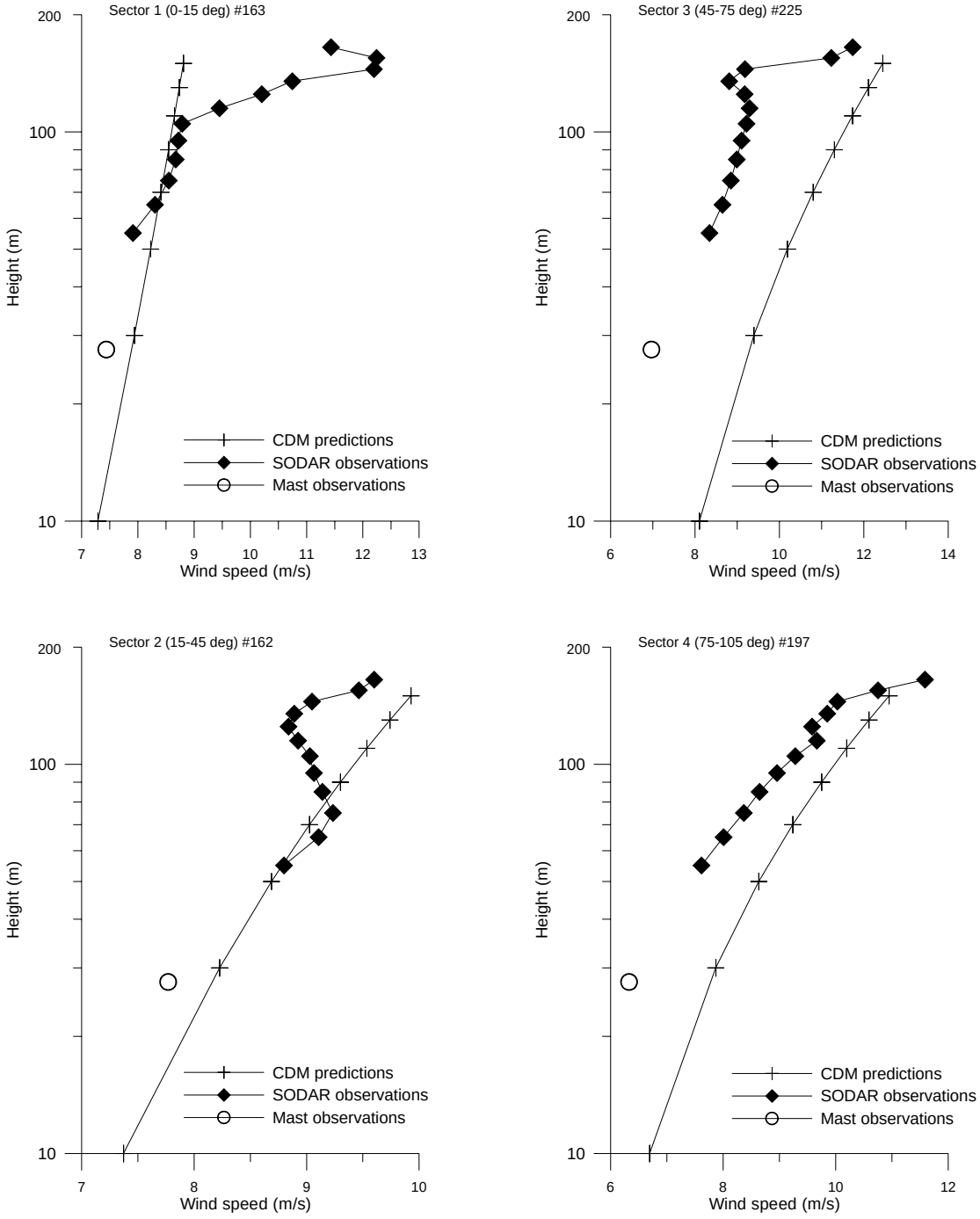

Figure 5-26. ***SODAR observed wind profiles and CDM predictions by sector. Also shown are mean wind speeds from the mast at MPN.***

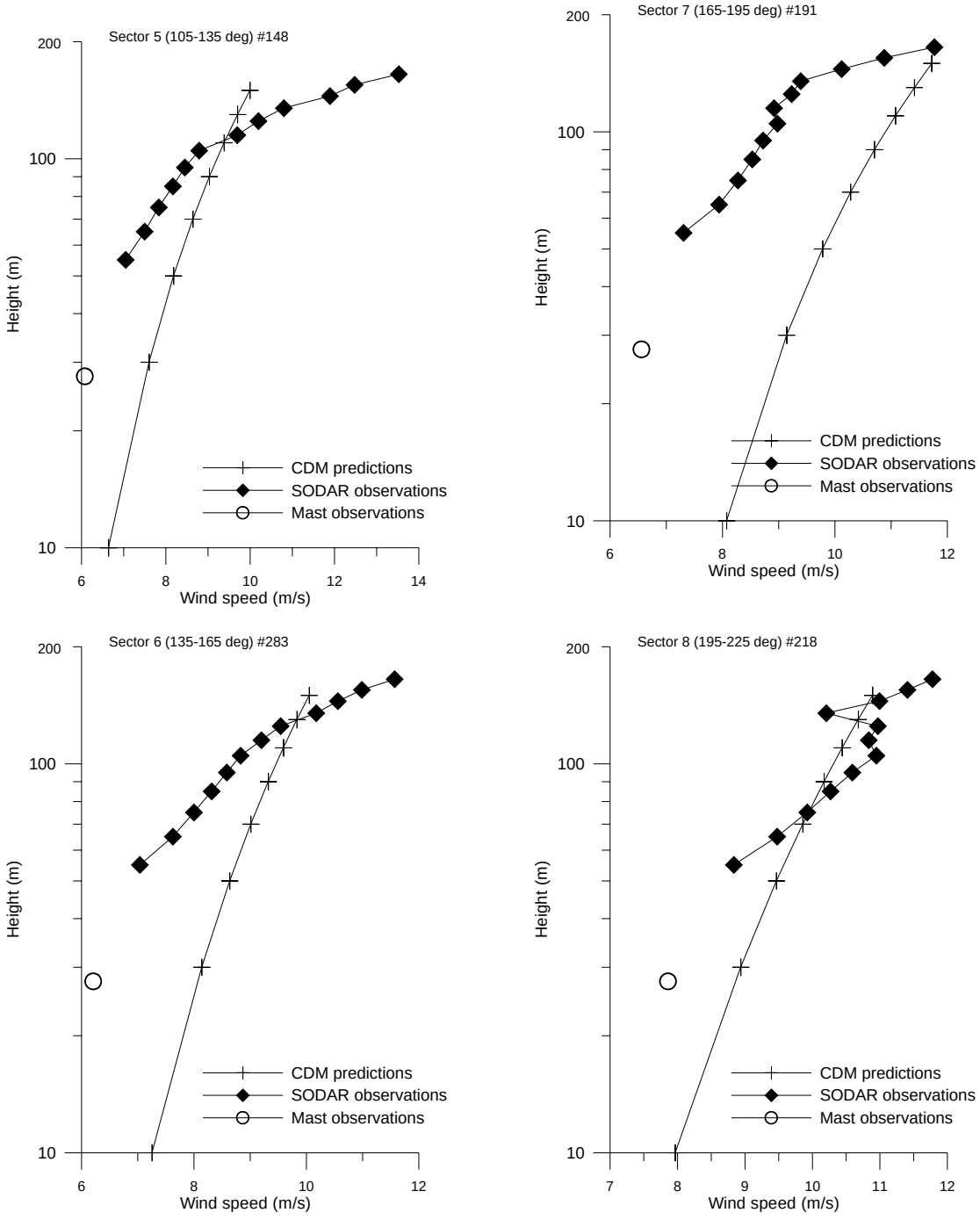

Figure 5-26. ***SODAR observed wind profiles and CDM predictions by sector. Also shown are mean wind speeds from the mast at MPN (continued).***

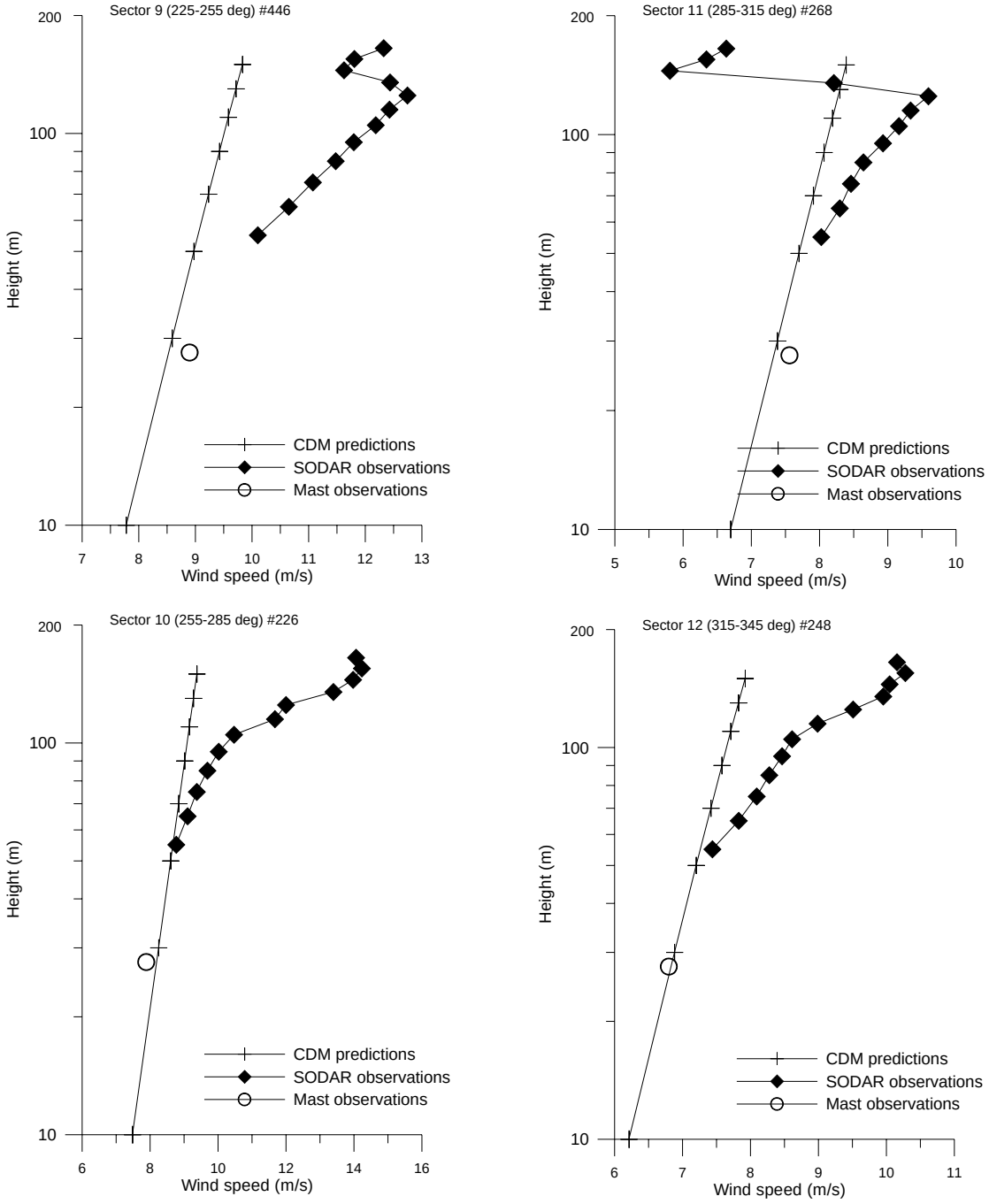

Figure 5-26. SODAR observed wind profiles and CDM predictions by sector. Also shown are mean wind speeds from the mast at MPN (continued).

In terms of stability Table 5-10 shows that the near-neutral class is not very frequent. Observations are divided between stable and unstable classes. Unusually both very stable and very unstable classes have relatively high mean wind speeds indicating a strong temperature profile at MPN.

Table 5-10-. Frequency of different stability classes

Stability class	L	Mean mast wind speed (m/s)	# Obs.	%
Very stable	0-200	6.6	726	26
Stable	200-1000	7.9	509	18
Near-neutral	±1000	7.1	213	8
Unstable	-200- -1000	7.2	326	12
Very unstable	0- -200	5.5	1001	36
Total			2775	100

Figure 5-27 shows the predicted and observed wind speeds in different stability classes. In the stable and very stable classes, the CDM predicts the shape of the profile well in comparison with the observed although the wind speeds are over-predicted in the very stable class. In the neutral and unstable classes the shape of the profile is not well predicted with the SODAR observed wind shear being higher than that predicted. In the Unstable classes the wind speeds are under-predicted in comparison with the observations.

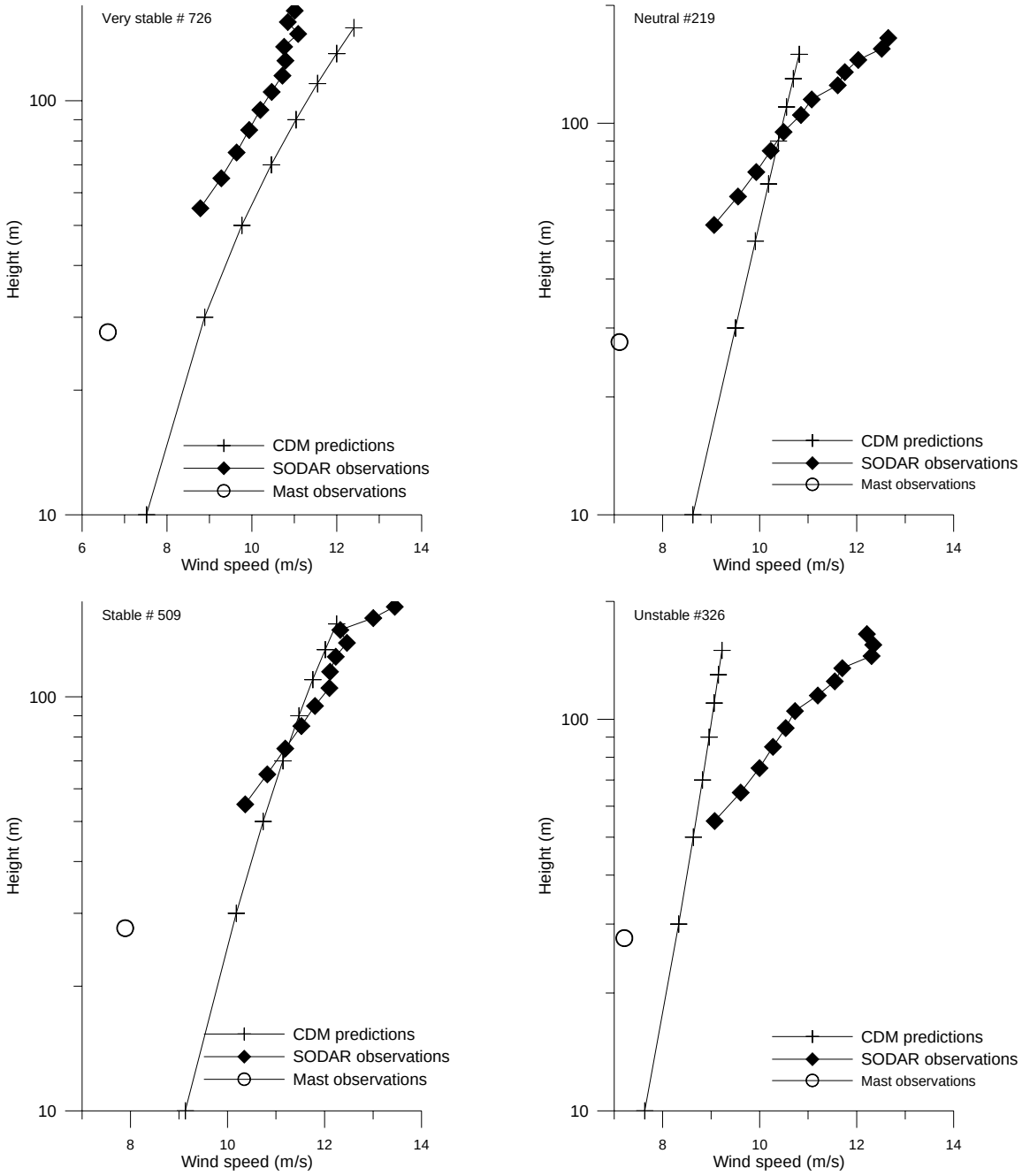

Figure 5-27. SODAR observed wind profiles and CDM predictions by stability class. Also shown are mean wind speeds from the mast at MPN.

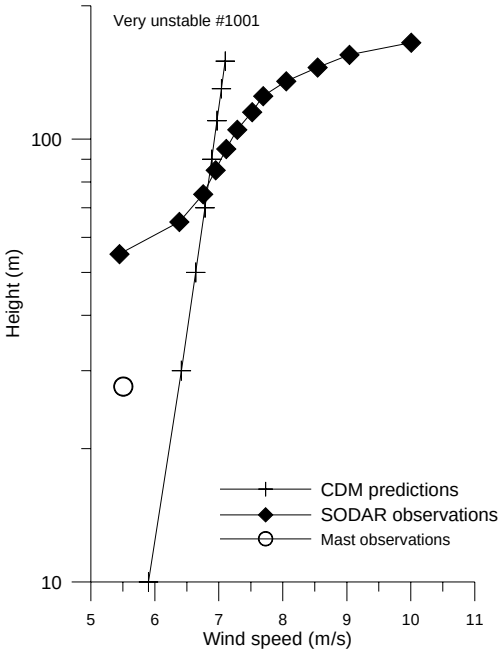

Figure 5-28. SODAR observed wind profiles and CDM predictions by stability class. Also shown are mean wind speeds from the mast at MPN.

Predictions can also be made based on observed wind speeds at Ijmuiden. For the period 24 Feb to 15 June 2001 the mean wind speed at IJmuiden is 6.41 m/s. The wind speed distribution and wind rose are shown in Figure 5-29. The wind direction is predominantly south westerly with components from the east and north east.

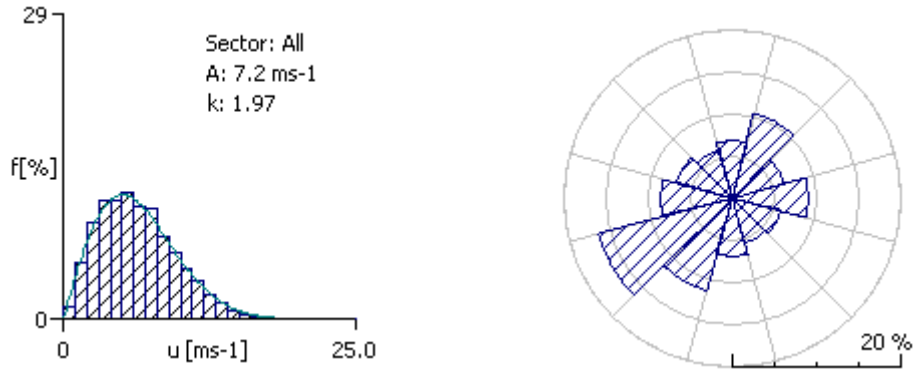

Figure 5-29. Wind speed distribution and wind rose from data at IJmuiden.

Predictions of wind speed at MPN were made using the CDM and data from IJM as outlined above for the period 24 February to 15 June 2000. As shown in Figure 5-30 this gives very similar results to predictions using data from HVH.

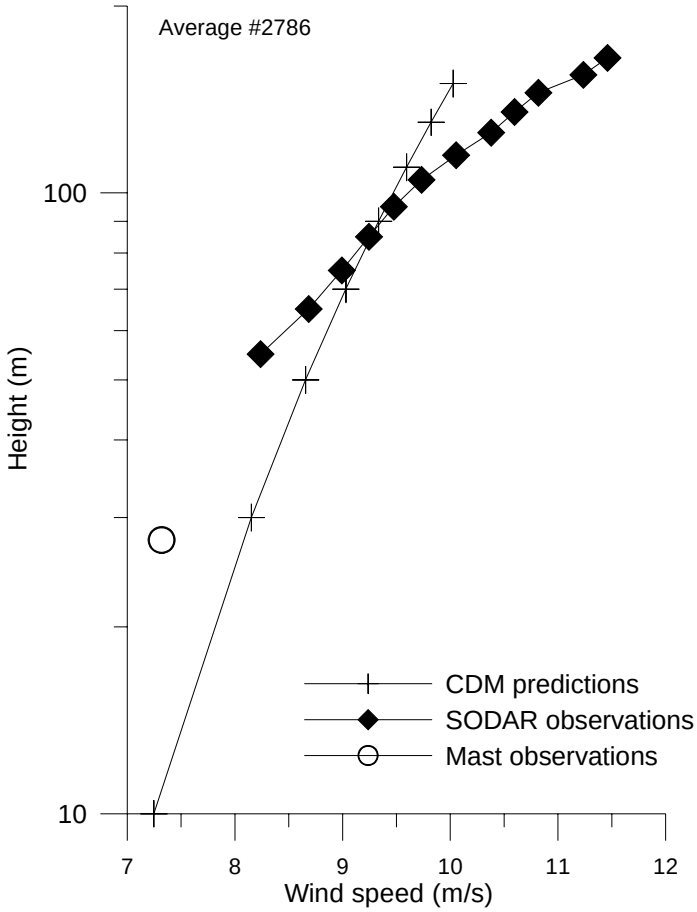

Figure 5-30. CDM predicted wind speeds and SODAR observed wind speeds at MPN.

As the problems in the predictions appear to be associated with the geostrophic predictions from the land sites a new approach was adopted for predictions from IJM, assuming that the site is surrounded by sea except in Sector 5 where the roughness length exceeds 0.002 m (Table 5-9). Predictions using this approach are shown in Figure 5-31. Although the predicted wind speeds are low compared with the SODAR there is good agreement with the mast wind speed. The wind speed profile predicted using the mast wind speeds (using the stability correction) shows the same general form as the CDM predictions. CDM predictions are higher because of the correction from IJM to geostrophic wind speeds. The form of the profile compared with the SODAR observations indicates that it is the thermal correction to the profile which is not correctly estimated using the temperature difference between land and sea. This can arise for a number of reasons - the estimated stability correction is highly sensitive to the temperature profile, here assumed to be the difference between two relatively small numbers. If this difference between two temperature sensors which are not calibrated together is slightly incorrect the stability profile at the site will be distorted. The large frequency of both stable and unstable classes rather than a dominance of one or the other would tend to indicate that this is not a problem so much as the relatively large temperature gradients. Further illustration of the stability classification at the site is given in Figure 5-32. Typically the number of observations in the near-neutral class increase with increasing wind speed. At this site, although the number of observations in the very stable or very unstable classes decrease with increasing wind speed, the number of observations in the near-neutral class does not increase. Figure 5-32 also shows the frequency of different stability classes by direction. Directions associated with a relatively short sea fetch have very few observations classified as neutral, with observations divided into the very unstable or very stable classes. This seems to reflect the influence of land at the site, giving large temperature gradients which are classified into the ‘extreme’ classes.

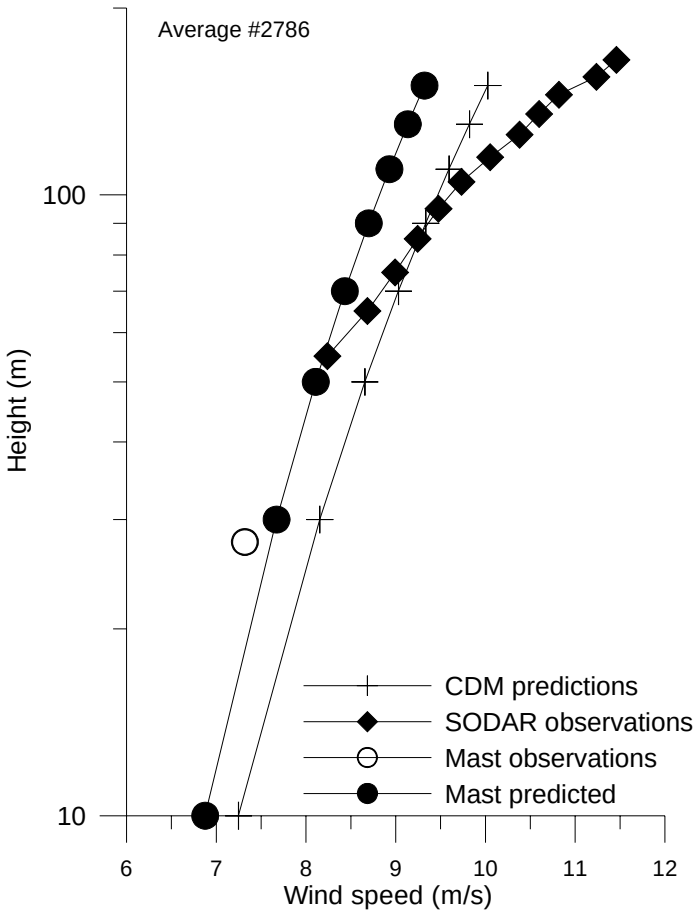

Figure 5-31. CDM predictions assuming IJM is an offshore site with only one land sector (sector 5).

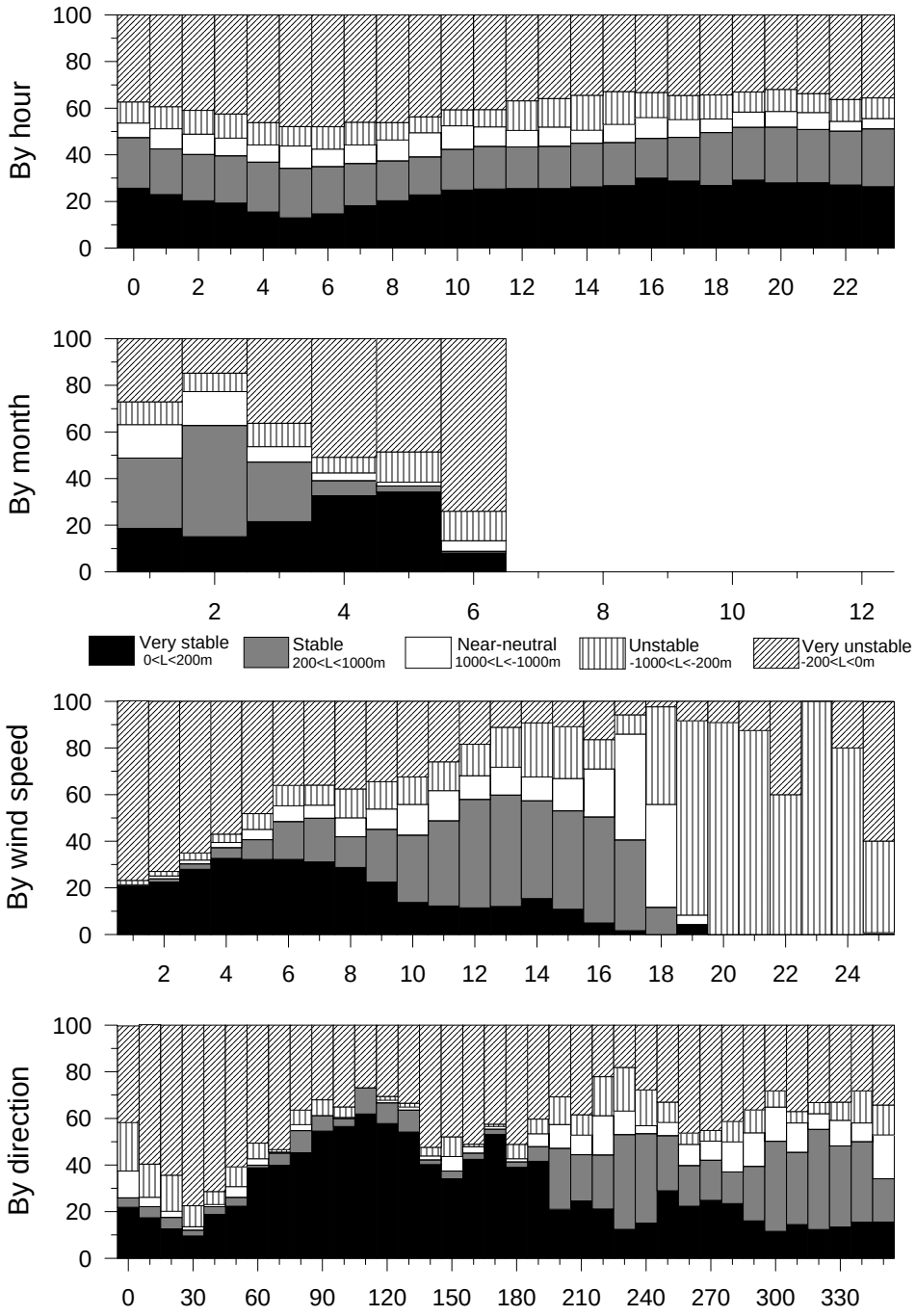

Figure 5-32. Classification of stability by hour, by month, by wind speed and by direction at MPN.

A comparison has been made between wind speed profiles observed by SODAR at MPN off the coast of the Netherlands and predictions using a coastal model (CDM) which accounts for stability variations in each observation. The CDM gives a good prediction of mean wind speeds at about 100 m height but over-predicts wind speeds below this height and under-predicts wind speeds at greater heights. Differences between the predictions and the observations are ascribed to two factors. Over-prediction of geostrophic wind speeds from land-based observations in sectors which have land fetch and greater wind shear than expected assuming a sea surface roughness of about 0.0002 m. Under-prediction of wind shear is ascribed to the stability definitions at the site which suggest that near-neutral conditions are comparatively infrequent while very stable and very unstable conditions dominate the observations.

5.4.3 Comparison of modelled and measured offshore wind speed profiles

Evaluation and comparison of the GEO-WASP, GEO-CDM and WASP-CDM focuses on offshore data collected at sites in Denmark (Figure 5-33). The data are collected on purpose-built meteorological masts offshore and are high quality wind speed profile data from a period of at least two years (except at Horns Rev and Læsø when one years data are available). The data record at Vindeby is the longest and most complete (over 91,000 observations) while that at Middelgrunden is the shortest (just over 21,000 records).

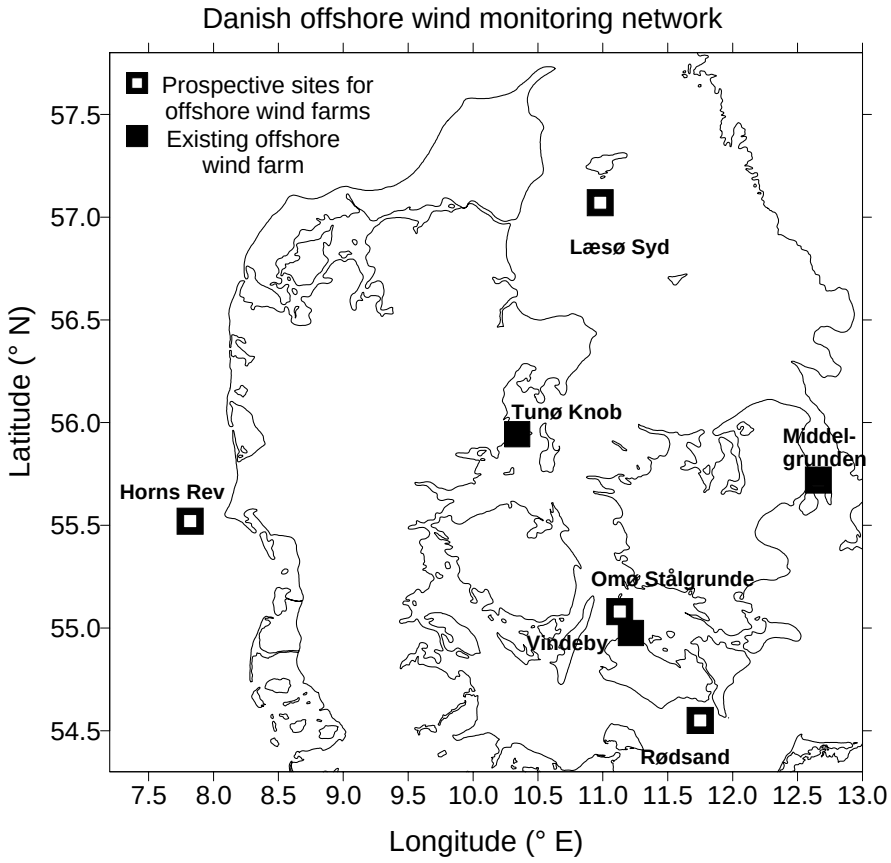

Figure 5.33. Danish Offshore Wind Monitoring Network

Editorial note : Unfortunately the analysis reported in the following section can not be published as the data was obtained under a non-disclosure agreement. The section and its associated figures 5.34-5.40 has been deleted from this PDF version.

5.5 Conclusions

The CDM and WAsP have been applied to the waters of the European Union based on geostrophic wind speeds and have been found to give reasonable predictions in comparison with mast and platform data. Typically all three methods evaluated (GEO-WASP, GEO-CDM and WASP-CDM) overpredict wind speeds in comparison with those observed.

Applying the CDM to WASP predicted wind speeds does not improve the predictions at all sites. The main reason for this is that a mean stability correction has to be applied to the wind speed distribution predicted by WAsP and this is not sufficiently accurate. Instead a time series of corrections should be calculated and applied prior to summarising the wind statistics.

The major problem with applying all three models appears to be with the spatial resolution and the calculation of the stability correction. The initial data sets are supplied on 0.5 by 0.5 ° grid whereas it is known that mean offshore wind speeds vary on scales of about 0.5 km in coastal regions. The CDM and WAsP applied at the 0.5 by 0.5 ° grid scale are unable to resolve complex coastlines (such as those around Denmark). Applying the same techniques with an improved coastline resolution would improve the predictions. In addition the use of air temperatures from mixed land/sea grid cells may not provide an accurate determination of stability, particularly when combined with a sea surface temperature data base from different sources. As noted above errors in the databases are of the same order as the temperature difference which is used to calculate the stability parameter. However to improve the stability correction is more difficult since a) currently sea surface and air temperatures are not available at better than 0.5 by 0.5° grid resolution and b) a more precise estimate of stability requires either direct flux measurements or a measured temperature difference.

5.6 References for Chapter 5

Barthelmie, R.J., 1999a: *Development of the Coastal Discontinuity Model*, Risoe National Laboratory, Roskilde.

Barthelmie, R.J., 1999b: The effects of atmospheric stability on coastal wind climates. *Meteorological Applications*, **6(1)**, 39-48.

Barthelmie, R.J. 2002: Evaluating the impact of wind induced roughness change and tidal range on extrapolation of offshore vertical wind speed profiles. *Wind Energy* (in press).

Barthelmie, R.J., Courtney, M.S., Højstrup, J. and Larsen, S.E., 1996a: Meteorological aspects of offshore wind energy - observations from the Vindeby wind farm. *Journal of Wind Engineering and Industrial Aerodynamics*, **62(2-3)**, 191-211.

Barthelmie, R.J., Courtney, M.S., Højstrup, J. and Sanderhoff, P., 1994: *The Vindeby Project: a description*. Risø-R-741(EN), Risø National Laboratory, Denmark.

Barthelmie, R.J., Grisogono, B. and Pryor, S.C., 1996b: Observations and simulations of diurnal cycles of near-surface wind speeds over land and sea. *Journal of Geophysical Research (Atmospheres)*, **101(D16)**, 21,327-21,337.

Barthelmie, R.J., Lange, B. and Nielsen, M., 1999*: Wind resources at Rødsand and Omø Stålgrunde.* Risø-I-1456(EN), Risø National Laboratory, Roskilde.

Barthelmie, R.J. and Palutikof, J.P., 1996: Predicting offshore wind speeds in coastal regions suitable for wind energy. *Journal of Wind Engineering and Industrial Aerodynamics*, **62(2-3)**, 213-236.

Beljaars, A.C.M., Holtslag, A.A.M. and van Westrhenen, R.M., 1989: Description of a software library for the calculation of surface fluxes. Technical report TR-112, KNMI, De Bilt, Netherlands.

Bergstrom, H., Johansson, P.-E. and Smedman, A.-S., 1988: A study of wind speed modification and internal boundary-layer heights in a coastal region. Boundary-Layer Meteorology, 42(4), 313-335.

Charnock, H., 1955: Wind stress on a water surface. *Quarterly Journal of the Royal Meteorological Society*, **81**, 639-640.

Coelingh, J., Folkerts, L., Wiegerinck, G. and van Zuylen, E., 2000: Study of the offshore wind climate using a SODAR, Offshore Wind Energy in Mediterranean and other European Seas. ATENA, Rome, Sicily, April 2000, pp. 61-70.

Coelingh, J.P., van Wijk, A.J.M. and Holtslag, A.A.M., 1996: Analysis of wind speed observations over the North Sea. *Journal of Wind Engineering and Industrial Aerodynamics*, **61**, 51.

Coelingh, J.P., van Wijk, A.J.M. and Holtslag, A.A.M., 1998: Analysis of wind speed observations over the North Sea coast. *Journal of Wind Engineering and Industrial Aerodynamics*, **73**, 125-144.

Donelan, M.A., Dobson, F.W., Smith, S.D. and Anderson, R.J., 1993: On the dependence of sea surface roughness on wave development. *Journal of Physical Oceanography*, **23(9)**, 2143-2149.

Garratt, J., 1977: Review of drag coefficients over oceans and continents. *Monthly Weather Review*, **105**, 915-929.

Garratt, J.R. and Ryan, B.F., 1989: The structure of the stably stratified internal boundary layer in offshore flow over the sea. *Boundary-Layer Meteorology*, **47(1-4)**, 17-40.

Geernaert, G., Katsaros, K. and Richter, K., 1986: Variation of the drag coefficient and its dependence on sea state. *Journal of Geophysical Research*, **91(C6)**, 7667-7679.

Johnson, H.K., Højstrup, J., Vested, J. and Larsen, S.E., 1997: On the dependence of sea surface roughness on wind waves. *Journal of Physical Oceanography*, **28**, 1702-1716.

Kitaigorodsky, S.A. and Zislavsky, M.M., 1974: A dynamical analysis of the drag coefficients at the sea surface. *Boundary-Layer Meteorology*, **6**, 53-61.

Mahrt, L., Vickers, D., Howell, J., Hojstrup, J., Wilczak, J., Edson, J. and Hare, J., 1996: Sea surface drag coefficients in RASEX. *Journal of Geophysical Research*, **101**, 14,327-14,335.

Mortensen, N.G., Landberg, L., Troen, I. and Petersen, E.L., 1993*: Wind Analysis and Application Program (WASP)*. Risø-I-666 (EN)., Risø National Laboratory, Roskilde, Denmark.

Nordeng, T.E., 1991: On the wave age dependent drag coefficient and roughness length at sea. *Journal of Geophysical Research*, **96**, 7167-7174.

Panofsky, H.A., 1973: Tower micrometeorology. In: D.A. Haugen (Editor), Workshop on micrometerology. American Meteorological Society, Boston, MA, pp. 151-176.

Pryor, S.C. and Barthelmie, R.J., 1998: Analysis of the effect of the coastal discontinuity on near-surface flow. *Annales Geophysicae*, **16**, 882-888.

Smedman, A.-S., Bergstrom, H. and Grisogono, B., 1997: Evolution of stable internal boundary layers over a cold sea. *Journal of Geophysical Research*, **102(C1)**, 1091-1099.

Smedman, A.S., Hogstrom, U. and Bergstrom, H., 1996: Low level jets - a decisive factor for off-shore wind energy siting in the Baltic Sea. *Wind Engineering*, **20(3)**, 137-147.

Smith, S.D., 1988: Coefficients for sea surface wind stress, heat flux, and wind profiles as a function of wind speed and temperature. *Journal of Geophysical Research*, **93(C12)**, 15467-15472.

Stull, R.B., 1988: *An introduction to boundary layer meteorology*. Kluwer Publications Ltd, Dordrecht, 666 pp.

Troen, I. and Petersen, E.L., 1989: *European Wind Atlas*. Risø National Laboratory, Roskilde, Denmark, 656 pp.

Van Wijk, A.J.M., Beljaars, A.C.M., Holtslag, A.A.M. and Turkenburg, W.C., 1990a: Diabatic wind speed profiles in coastal regions: comparison of an internal boundary layer (IBL) model with observations. *Boundary-Layer Meteorology*, **51**, 49-75.

Van Wijk, A.J.M., Beljaars, A.C.M., Holtslag, A.A.M. and Turkenburg, W.C., 1990b: Evaluation of stability corrections in wind speed profiles over the North Sea. *Journal of Wind Engineering and Industrial Aerodynamics*, **33**, 551-566.

Wieringa, J., 1986: Roughness-dependent geographical interpolation of surface wind speed averages. *Quarterly Journal of the Royal Meteorological Society*, **112(473)**, 867-889